ÉCOLE POLYTECHNIQUE
FÉDÉRALE DE LAUSANNE

A Neural Visuomotor Controller for a Simulated Salamander Robot

Biljana Petreska
`biljana.petreska@epfl.ch`

EPFL / Computer Science

Diploma Thesis
February 2004

Responsible
Prof. Auke Jan Ijspeert

EPFL / BIRG

BIOLOGICALLY INSPIRED
ROBOTICS GROUP (BIRG)

Abstract

This work investigates the neural circuitry underlying visually-guided behavior in salamanders, with a special attention to the interplay of neural processing and the biomechanics of the vertebrate body. The aim is to gain more insights on how visual information is encoded in the brain and transformed into motor controlling signals. It presents topological mappings between the optic tectum and the brain stem that produce accurate estimates for prey localization.

Models of the amphibian retina, optic tectum, pretectum and tongue protraction are built upon a previous simulation of the neuromechanical salamander locomotion developed by Ijspeert, capable of exhibiting the typical swimming and stepping gaits of a salamander. The developed models reproduce extensive biological lesion data and account for several particular behaviors, such as generation of saccadic movements, bending approach within monocularized salamanders and explain observed prey preferences. The simulation environment is an appropriate tool for testing any contribution related to neural visuomotor coordination, since it was adapted to display the brain neural activity.

This research area is relevant for *neural computing* - where the aim is to develop ideas from neuroscience into a form that is promising for the development of *perceptual robotics* - and *computational neurobiology* - in which models are developed which stand or fall in relation with the experimental biological and neurophysiological data.

Contents

Chapter 1

Introduction

The aim of this project is to investigate, through simulations tightly coupled with data from extant and new experiments, the neural mechanisms underlying visually-guided behavior in vertebrates.

We believe that bridging between computer and cognitive sciences could overcome present barriers to the "true" intelligence in artificial systems. The initiative aims at decoding brain processes (a sort of "reverse engineering" of the brain) and assign meaning to complex patterns of sensory stimuli. Not only it is relevant for *perceptual robotics*, but it presents a test bed for probing the accuracy of *neurobiological considerations.*

The project is focused on an amphibian preparation, the salamander, which provides in a sense a Bauplan for vertebrates in general. The relative simplicity of neural circuitry in the salamander brain renders it tractable from an experimental point of view. The controller presented in this project is not a "traditional" robot controller in the sense that it deals rather poorly with obstacle avoidance. We were primarily interested in giving insight on how visual information is decoded in the brain and coordinates motor controls. The addressed question was to investigate potential mappings between the optic tectum, i.e., the main visual processing brain area, and the brain stem, which comprises the premotor and motor centers of the salamander. A structured projection pattern was to be considered with respect to feeding and visual tracking behavior. Subsequently it was extended to various functional subsystems underlying visuomotor coordination in amphibians, such as predator avoidance and depth perception.

We have built upon a neuromechanical simulation of salamander locomotion developed by Ijspeert, capable of exhibiting the typical swimming and stepping gaits of a salamander. It includes a bio-mechanical model of the body, and a leaky-integrator neural network model of locomotor spinal circuits. A preliminary study [18], demonstrated that the locomotor CPG could produce stable rhythmic patterns despite the rapidly changing input signals.

1.1 Addressed Questions

The primary questions addressed are [16]:

- How can the stimulus localization and depth estimates be extracted from the tectum maps?
- What sensorimotor transformations occur at the level of the optic tectum, the brainstem and the pathways between them? Can a structured mapping provide an accurate a sensorimotor transformation?
- How are the body and neck movements coordinated during the approach towards a stimulus?
- How is the visual perception influenced by head motion during the approach toward a stimulus? Are additional mechanisms necessary for dealing with the remaining shifts in the visual background?
- Which type of a tectum-brainstem mapping explains the typical curved approach in monocularized salamanders?
- Which mechanism implements the release of the snapping behavior? and how is the tongue controlled?

1.2 Reminder

The reminder of the report is as follows: in Chapter 2 we give a concise but complete review on the state of the art on the salamander's visually guided behavior. The aim was to provide a practical summarizing text which would combine many different literature sources. In Chapter 3 we provide an overview of several previous works on the subject. Chapter 4 describes the models used and developed within this project and Chapter 5 presents respective results. Finally, Chapter 6 concludes the report.

Chapter 2

A Literature Review

A considerable amount of data has been accumulated on behavior, neurophysiology and neuroanatomy related to visually guided neural mechanisms in salamanders. We were somewhat attributed the task to summarize and integrate information from different literature sources. This section is rather exhaustive and was aimed to provide a serious and useful background knowledge for further projects on visuomotor coordination in amphibians.

2.1 Salamanders

Salamanders belong to the reign of amphibians. There are three orders, 37 families and 3924 species indexed so far. They have invaded most diverse habitats and can be found on almost all continents. Salamanders are fascinating animals. They show a great variety of lifestyles, as some species are permanently aquatic and other sedentarily terrestrial. Some of them undergo a complete metamorphosis, while others stay in larvae state. Their size can vary from exceptionally large to unusually small, giant salamanders measure up to 150 cm (*Andrias*), whereas the adult *T.pennatulus* is 16 mm long. Their aspect can be very different: the *Amphiumidae* is an eel like species, the *Typhlotriton* is blind and unpigmented, the *Batrachoseps* is a four-toed wormlike salamander and the *Lineola* is in semi-fossorial form. By adapting themselves to the living environment, some salamanders have developed very interesting properties (secreting a moisture sealing cocoon over their body to survive droughts) and highly specialized feeding mechanisms (some urodeles have the greatest tongue length with respect to their body). For some more taxonomy, geography and ecology of salamanders please refer to the source of the aforementioned information [26, p. 273]. Most frequently referred species in the paper will be the *Hydromantes Italicus* from the *plethodontid* family and the *S.salamandra* from the *salamandridae* family genus (also known as fire salamander) since there is a lot of data available on their subject and the latter was the primary inspiration to the salamander locomotor circuit and the salamander robot 2.1.

Figure 2.1: S.salamandra and the Birg Salamander Robot.

2.2 Visually Guided Feeding Behavior

Salamanders possess an unusual variety of sensory mechanisms for the detection of prey. These include vision, olfaction, vibration sense, mechanoreception, and electroreception by means of the lateral line system [26, Chapter 2]. Except for a number of aquatic salamanders which are totally blind as adults and must rely on non-visual mechanisms, or under adverse environmental conditions such as muddy water, dark nights or underground, vision is by far the most important sense involved in the guidance of feeding. The visual sense is predominant and visual cues override for example the olfaction sensory perceptions under daylight conditions (i.e., the animal will be dubious about the olfaction signals if it can not see the source and will not hesitate in the dark [26]).

2.2.1 Feeding strategies

There are two distinct types of feeding [26, Chapter 2]. Aquatic salamanders gape and suck a rapid inflow of water including the prey item. Terrestrial salamanders protrude their tongue out of the mouth such that the prey is caught primarily by gluing it onto the tongue pad. For large prey items or prey possessing defensive mechanisms they combine also the use of teeth and jaws. As we will see below the abolition of both aquatic larval stage and lung-breathing has lead to highly specialized feeding mechanisms (e.g., ”ambush” strategies).

In terrestrial salamanders there is a close connection between the sensory guidance of feeding behavior, the behavioral feeding strategy, and the functional morphology of the feeding apparatus [26, Chapter 2]. A salamander with an unspecialized, massive tongue of short range will prefer ”hunter” strategies (i.e., actively search for prey). The visual system of these animals is rather poor: they have a small number of retinal neurons, less frontally oriented eyes and no substantial direct ipsilateral input (i.e., input from the second eye). *S. salamadra* for example has the least developed tongue with regard to the distance of its protrusion and its effectiveness of hitting the prey (success rate of 39%). As they snap in more or less frontal direction, they have to orient their head directly toward the prey.

A very specialized, greatly extendable and high speed tongue makes feeding on fast moving objects through the use of low energy ”ambush strategy” possible (i.e., waits for the prey to come close before snapping it), but this system requires more highly evolved capabilities of the visual system, with regard to prey localization and depth perception. The most specialized tongues of all sala-

Figure 2.2: H.Supramontis capturing a house fly with its projectile tongue

manders with regard both to velocity and distance are found in species of the genus *Bolitoglossa*. In some species the tongue is protruded out of the mouth to its full length of 20-25 mm (up to 80% of the body length) in 2-4 ms (see picture 2.2). *Hydromantes Italicus*, possesses by far the longest tongue with reach of 45-50 mm, the protrusion lasts 6-8 ms and the retraction is slower with 80-100 ms. *Bolitoglossini* are able to shoot their tongue laterally, sometimes at an angle of 45°. For impressive movies of salamander feeding refer to [10].

In addition some salamanders are are known to switch from one strategy to another depending on prey density or prey type (Jaeger 72) in [28]).

2.2.2 Sequence of feeding behavior

The first reaction to a prey object is a turning movement which permits to the salamander to fixate the object binocularly. Salamanders perform the initial **orienting movement** with the head alone (not with the whole body). Then the salamander **approaches** the prey by walking toward it until it is within reach of the jaws or tongue. There is only a little approach in salamanders with "ambush" strategy. An **olfactory test** may occur when the prey is within reach. During this reaction salamanders show a characteristic posture which increases the frequency of ventilation movements and helps to suck the odor substances into the olfactory organ. After reaching a snapping distance, salamanders usually **fixate** the prey object binocularly for a shorter or longer period depending on its attributes such as movement intensity. Gaze stabilization reaction is species specific. By **snapping**, the prey is finally seized onto the protruded tongue and taken into the mouth. Information about sequence of prey-capture behavior reactions have been gathered from [26].

Study of visual prey recognition in amphibians has suffered from two incorrect assumptions in the past [28]. A first incorrect assumption on salamander feeding was that capture of prey by amphibians is a stereotyped behavior or "fixed action pattern"(Tinbergen 51) which is triggered by an invariable "sign stimulus" interacting with "feature detectors" in the visual system which then as "command elements" release the feeding response (Ewert 68) (i.e.,behavioral sequence is released more-or-less automatically by objects fitting a relatively simple prey scheme, i.e. objects that move and are not too small or too large to be eaten or objects that exhibit simple configuration properties (Lettvin et al., 1959; Grüsser and Grüsser-Cornehls, 1976; Ewert, 1984, 1989) [29]). For example, if the prey is removed during a critical phase of fixation, toads snap accurately at the empty stimulus site (Hinsche,1935), and the subsequent gulping and mouth wiping also occur (Ewert, 1967) [4]. However, prey capture in amphibians is not stereotyped, as they can regulate their tongue protrusion with respect to their feeding strategy and to the distance and velocity of prey (Maglia and Pyles 95). There is clear evidence that, in amphibians, both visual and non-visual prey recognition is experience-dependent [29]. Neither there are invariable properties that act like sign stimuli. The feeding sequence can stop at any point (vs. stereotyped). Basic neural units for prey recognition are no more regarded as specific single, retinal "detector cells", but are more likely the result of a mass-combined (e.i., overall-simultaneous) activity of different kinds of cells within smaller or larger networks and with partly overlapping response characteristics.

2.2.3 Prey Preferences

The second incorrect assumption was that because salamanders eat such diverse sizes and species of prey they are commonly believed to indiscriminately ingest whatever prey they encounter (Hairston,49,80), limited only by the morphological constraints of their visual system and feeding apparatus (i.e. they feed on everything that moves and is not to small to detect and not too large to swallow). From this and the fact that relatively simple artifacts (dark rectangles on a white screen) may elicit an orienting behavior, it was concluded that amphibians can not discriminate between different kinds of prey due to their incapacity to recognize objects. However, they appear to follow the rule "take and try it and store the result". When amphibians are allowed to ingest cardboard dummies, they spit them out and lose interest in these objects (Göckel, 2001) [29]. In orienting experiments with dummies, animals snapped at the screen only once in a session and at the beginning of the experiment, but fed immediately or with a short delay when live crickets were presented randomly between stimulus presentations [29]. There are also well-documented cases in which salamanders make subtle distinctions between different kinds of prey with respect to their *size*, *velocity*, *configuration and orientation*, *movement pattern*, *stimulus-background contrast*, *nutritive value*, *digestibility* and *potential harmfulness*. Moreover these parameters are inter-dependant (i.e., they yield different behavior patterns when alone or combined) and depend on internal motivational or attentional states and individual experience [29].

In a Salamander Stomach

What a salamander eats is in the first place determined by the availability and abundance of prey within its natural habitat. The actual composition of the food found in their stomach does not necessarily reflect the true preferences of the animal under study. Here is a short overview of what can be found in a salamander stomach. Salamanders are exclusively carnivorous animals. They eat all kinds of insects (coleopterans, houseflies, crickets, mites), gastropoda (different kinds of slugs and earthworms, ants and millipedes), invertebrates (aquatic insects, mollusks and crustaceans) and larvae (tadpoles) [26]. Large salamanders are voracious eaters and commonly feed on large preys such as rats, mice, turtles, snakes and even birds [28]. The broad-headed morph is cannibalistic and most of his diet (84%) consisted of other salamanders.

Stimulus Size

According to [29] prey size seems to be one of the most important features eliciting orienting responses. In this study by on orienting behavior of *Plethodon Jordani* the large-sized cricket (15 mm) was most preferred by all individuals and the small-sized cricket (6 mm) was among the least-preferred stimuli.

There is no correlation between the salamander head width and prey size (Lynch, 85 and Roth,74) [26]. Lower size limits are identical and independent of the salamander body size or head width. Larger salamanders eat increasingly larger preys, but continue to eat smaller prey. Except for *Bolitoglossini* who eat only small prey because they exclusively feed with their tongue and have difficulties in feeding on large and elongate prey stimuli (which have to be taken completely into mouth when tongue is returned). Thus there is a correlation between the morphology of the feeding apparatus and the prey size spectrum. An idea of prey size range can be found in Table 2.1. One important aspect is that many amphibians do not maximize size prey. Preferred size is not identical with maximally devourable size, the threshold is not fixed and fluctuates with changes in the internal and motivational state of the animal. For example in the frog Bufo fowleri, the upper size threshold of prey eliciting feeding behavior was reduced when the toad fed and became satiated (Heatwole, 1968) [29]. Another important aspect is that salamanders often snap at stimuli that are far too large to be swallowed and have difficulties with ingesting the prey [3] and [26], which corroborates the assumption of salamanders having a rather poor depth estimation (i.e., have difficulty with evaluating the absolute size which is a function of the prey angular size and its distance).

Stimulus Velocity

Movement is almost a necessary prerequisite in the sense that motionless objects are usually ignored and not interpreted as prey. According to [29] it is the second dominant feature for determining stimulus preferences (after size). Preferred velocities are listed in Table 2.1. It is worth mentioning that *Bolitoglossa rufescens* has extremely fast feeding reactions and catches flies on the wing at angular velocities of about 300°/s [28]. Local motion is of little importance, but still elicits orienting movements [29].

Stimulus Shape

Salamanders are clearly able to discriminate between stimuli of different shapes and orientation with regard to the direction of movement ("worm" and anti-worm" shapes) [28]. Shape preferences are highly species dependant, reflecting their natural diet. *S.salamandra*, shows a strong preference for worm-like stimuli, while *plethodontid* salamanders prefer compact prey object such as insects [26]. Salamanders snap at the leading edge of the object, rather than at the object itself (Luthard, 1981) [26]. According to [29] shape was of intermediate importance.

		Minimum	Maximum	Optimal
S.salamandra	Size	2 mm	16 mm	32 mm
	Velocity	0.5°/s	5-15°/s	40°/s
H.Italicus	Size	0.5 mm	1-5 mm	10 mm
	Velocity	0.24°/s	4.8-72°/s	172°/s
S.Salamandra	Size	1°	4-10°	20°
	Velocity	0.5-1°	5-20°	40-110°/s

Table 2.1: Stimulus size and velocity preferences for *S.salamandra* and *H.italicus* from [26, pages 35-36] and [13]

.

Movement Pattern

Forward movement of an object appears to be important for eliciting an orienting response [29] and prey dummies increase in attractiveness, as their movements become more irregular [26]. Movement pattern interacts in a complex manner with velocity and seems to be connected with a certain shape. It has been suggested that salamanders associate an elongate, "wormlike" shape of a stimulus with slow and smooth movement, and that they associate a compact shape of a stimulus with a fast and discontinuous movement [26]. Movement pattern is of intermediate importance [29] and seems to be an important cue in darkness [26].

Stimulus-Background Contrast

In the study on preferred stimulus for orienting movements of *Plethodon Jordani* the contrast-reduced cricket evoked fewer responses than most of the other stimuli [29]. Therefore contrast is another important feature in eliciting orienting responses.

Experience-Dependant

Salamanders learn to avoid noxious or unpalatable prey like bumblebees, honey bees or wasps (after one or very few trials) (Cott, 1936; Sternthal; 1974; Dean, 1980) [26]. Different individual experiences contribute to modified patterns of prey preference. When salamanders were tested singly, two individuals showed a significant effect [29].

Visual Attention

Salamanders follow the stimulus that they respond to first and do not switch to other moving stimulus, irrespective of their nature. [29]

Blind to stationery objects?

"A frog would starve to death in a heap of dead flies". However this does not seem to apply to salamanders. Even if they usually do not pay attention to stationery objects (i.e., they turn away from the object or snap at it as it moves again), they can be trained to respond to them [26]. Tremorlike eye movements

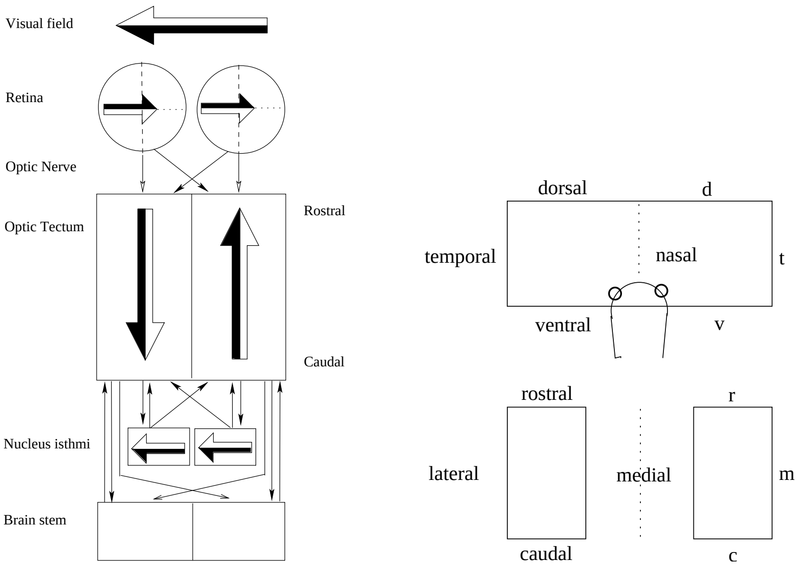

Figure 2.3: The flow of visual information to the motor centers in the brainstem. The arrows represent the direction of the topographic representation. On the right. Sides terminology.

demonstrated by Manteuffel (1977) would be sufficient to make a stationery prey visible.

Paired Stimulus

When presented with two stimuli moving in opposite directions, salamanders respond to 45% of the presentations of identical stimuli, whereas failures occurred in only 5% of paired-stimulus presentations with different stimuli. The difficulty of animals in responding to one of two identical stimuli may indicate a conflict of interpretation. The sensory information about the two stimuli is identical and can lead to equivalent excitation in the two tectal hemispheres which in turn blocks a visuomotor response to the stimulus [29] (see section 2.3.2).

2.3 Morphology and Function of the Salamander Brain

The salamander brain is composed of 5 parts: telencephalon, diencephalon (thalamus and preatectum), mesencephalon (tectum opticum, tegmentum and nucleus isthmi), cerebellum and medulla oblongata (motor nuclei of nerves) [28]. The mentioned areas will be described in this section.

The visual input enters through the *retina*, and is transferred to the brain via the *optic nerve*. The signal is retinotopically projected to the main visual processing center, i.e., the *optic tectum*. The optic tectum projects through the crossed and uncrossed tectobulbospinal tracts (i.e., *medulla oblongata* pathways)

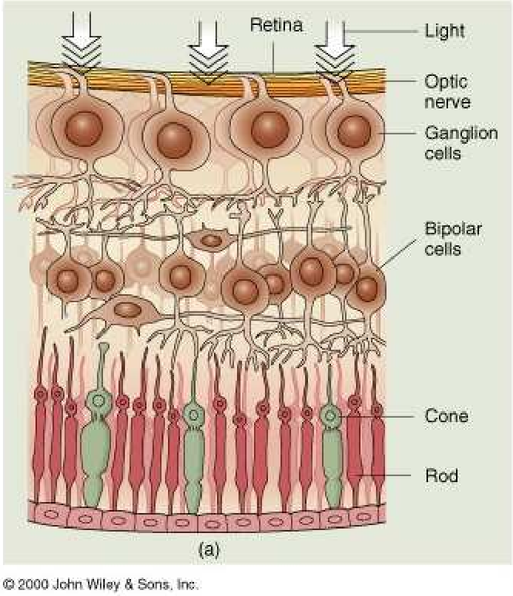

Figure 2.4: Organization of the Retina

to the *nucleus isthmi* and the brainstem, the latter contains the premotor and motor centers. The visuomotor information flow is illustrated in figure 2.3.

2.3.1 Retina

The retina is a filmy piece of tissue, barely half a millimeter thick, that lines the inside of the eyeball. Intuitively, one might expect that the surface of the retina (the layer exposed to the liquid in the eyeball's vitreous chamber) would contain the sensory cells, the *photoreceptors*, but actually these cells lie at the very back of the retina; light rays must pass through the entire retina before reaching the pigment molecules to excite [21]. From the photoreceptors (i.e., *cones* and *rods* responsible respectively for daylight and for night vision) signals pass through a series of intricate neurons connections (*horizontal*, *bipolar* and *amacrine* cells) toward the surface of the retina where the *ganglion-cell* nerve-fiber layer relays the processed visual information through the optic nerve into the brain. The preceding is illustrated on figure 2.4. More detailed and well presented information is available on [25].

The visual image from the eye is not simply impressed on the retinal surface and transmitted to the brain, as it has been assumed for a very long time. The retina performs a first stage of visual processing. Retinal ganglion cells are functionally differentiated (the visual signal is split in different channels that convey different information) and project to the primary cortex (i.e., optic tectum) through different visual pathways. We will interest ourselves on retinal ganglion cells which are the final layer of visual processing in the retina and basically form the visual input to the brain.

Retinal Ganglion Cells in Salamanders

Together with receptors, ganglion cells are most studied retinal neurons. Numbers of retinal cells that project to the optic nerve range from 26 000 to 75 000 (53 000 for *S.salamandra* and 47 000 for *H.Itallicus*) [28]. Different classes of retinal ganglion cells can be distinguished by the size of their excitatory receptive field ERF and inhibitory receptive field IRF; response to on-off diffuse illumination; response to stationary or moving stimuli of different velocity, size, shape and background contrast; and response to stimulation with light of different wavelengths. By receptive field of a neuron we mean the subset of the sensory space in which an appropriate stimulus elicits a reaction in the corresponding neuron. Excitatory or inhibitory represent the reaction to light.

Response Types of Retinal Ganglion Cells

Studies on retinal ganglion cells in *S. salamandra* (by Grüsser-Cornhels and Himstedt in 1976 as described in [26, Chapter 5]) have revealed three different retinal ganglion units. There is contradictory data on **Type 1** units receptive fields size. The aforementioned have found values such as 12 to 16 degrees of visual field. However these values are too large to explain the preferences of these cells for stimuli with 2-3° angular size [26]. These cells have a strong inhibition surround [28] and they do not respond to on-off changes in diffuse light. There is a short activation period after a change in the position of moving stimuli. Horizontal stimulus shapes were preferred over square or vertical (i.e., "wormlike" stimuli, rectangles oriented parallel to the direction of movement). **Type 2** cells have excitatory receptive fields of 6-9°. They respond with a short on-off activation to a change of diffuse light, possess a relatively weak surrounding inhibition and prefer slightly larger stimuli than the previous. They do not respond to velocities below 2 degree/s. The discharge rate increased with increasing velocity of stimulus. Neuronal activity increased also with increasing contrast between stimuli and background with a minimal contrast of 0.25[1]. They respond best to square objects or objects with vertical extension. **Type 3** cells have large excitatory fields of 10-20° with weak surrounding inhibition and exhibit tonic on-off responses to a change in diffuse light. Optimal responses are best achieved with large stimulus sizes. They respond well to slow stimulus velocities such as 0.05°/s and the increase of discharge rate is less strong with the increase of the stimulus velocity. They are much more contrast sensitive with a minimum threshold at 0.05. There is a clear dominance of square stimuli and least preferred are horizontal stimuli. These cells respond best to larger stimuli. You can find a short summary of S.salamandra retinal ganglion cells responses in Table 2.2.

Retinal Ganglion Cells Projections

Experiments with intracellular staining of retinal ganglion cells in salamanders [35] show that retinal ganglion cells have multiple terminal structures in the thalamus, pretectum and tectum. Retinal ganglion cells with an obvious dense terminal arborization in the pretectal neuropils show a great variation in size and structure. They do not project to the tectum.

---

[1] Measure of contrast: C = $(I_s - I_b)/(I_s + I_b)$ where I_s is the stimulus luminance and I_b is the background luminance.

	Type 1	Type 2	Type 3
ERF	2°-3°	6°-9°	10°-20°
IRF	strong 12°-16°	weak inhibition	very weak
change in light	no response	short activation	tonic response
minimal velocity		2°/s	0.05°/s
minimal contrast		0.25	0.05 saturate
size preferences	small	medium	large
shape preferences	H > S = V	S = V > H	S > V > H
tectum terminals	tectal layer 1	tectal layer 2	tectal layer 3
depth in tectum	5-15%	15-50%	50-70%
terminal arbors	100 μm	180 μm	400 μm
sensitive to	local contrasts	motion	overall illumination
function	edge detectors	detect motion	dimming detectors

Table 2.2: Properties of retinal ganglion cells in *S.salamandra*.

The terminals of retinal ganglion cells in the fiber layer of the tectum are spatially restricted to single laminae [33]. They project to three different layers. The terminal arbors in the most superficial *tectal layer 1* are small (average diameter of 100 μm) and round shaped. There is a massive dendritic overlap of adjacent cells [32]. They respond to changes in contrast and size of small objects and are probably concerned with detection and calculation of local contrasts (edges) [26]. Retinal arbors projecting to the intermediate *tectum layer 2* are antenna like fibers of 180 μm width and have also terminal arbors in thalamus and pretectum. There is also a high overlap of receptive fields. They possess thick myelinated (i.e., fast conducting) retinal axons which may indicate a temporally sensitive processes such as calculation of speed and movement direction. As they respond best to moving objects, they are probably concerned with the detection of movement and calculation of trajectories (Mandon et Roth 97). Layer 3 retinal terminals have moderate branching, 400 μm wide arbors (oval, flat and wide) and project densely in pretectum and thalamus. They overlap with the previous type. Larger arbors may indicate that they are not necessarily dependant on a precise visuotopic map. They are presumed to be involved in the overall change in luminance [26]. Thus, they are considered to be predator early warning devices used in escape behavior (likewise Maturana et al.(1960) *dimming detectors*, Grüsser et al.(1964) *OFF units*). However (Mandon and Roth 97) have shown a great variety of complex RGC3 response properties (i.e., they are heterogeneous with respect to their response properties) [6], which may indicate more complex tasks than just calculation of luminance. In salamanders, one subclass is sensitive to slow motion [6] and others are direction-selective mainly with respect to temporonasal and approaching movements.

2.3.2 Optic Tectum

The tectum is the primary visual system although calling it optic is un oversimplification as it integrates multimodal perception. The interaction between visual and nonvisual (e.g., ascending somatosensory, auditory, and vestibular) input onto efferent tectal cells is unknown. However, it is reasonable to assume that the information leaving the tectum through the ascending and descending pathways is not identical with the information carried by the different types of retinal input onto tectal efferent neurons. In Salamanders the optic tectum is directly connected to the motor and premotor centers and reaches reach more spinal levels than in frogs, reptiles or birds [6]. It acts as a releaser for behavior [28].

The optic tectum has multilayered appearance. The first three layers are retinorecipient layers, layers 4-5 are efferent fibres and afferents from other senses, layer 7 are deep unmyelinated fibres, 8 deep cellular layer and 9 glial cells [28]. the anatomical stratification of the tectum corresponds to different physiological properties. The three types of retinal ganglion cells (see section 2.3.1) project at a given depth and to a single laminae. The location of the different types of terminal arbors corresponds to the physiological subdivision of the tectal fiber layers (type 1 of retinal ganglion cells projects to tectal layer 1, etc.) [4]. The ipsilateral retinal input projects between layers 3 and 4 [28].

There is a topographic projection of the retina on to the tectum (i.e., neighboring objects in the visual field stimulate nearby objects in the optic tectum) [4]. Each visual hemifield is projected completely on the contralateral tectal hemisphere. However the visual image is inverted: the naso-temporal axis in the visual field corresponds to the rostro-caudal axis in the tectum and the dorsoventral direction in the visual field corresponds to the medio-lateral axis in the left tectal hemisphere and to the latero-medial axis in the right tectal hemisphere (see figure 2.3). This particular disposition is probably used in depth estimation 2.4.

According to Grobstein (1988) the tectum does not contain a global motor map, but instead is a relatively early stage within the visual information-processing sequence. Given the multiplicity of cell types in the tectum, it is better to think of it as providing a set of partial (overlaid [2]) maps, rather than a single map of any description [4].

Classification of Tectal Neurons

The intracellular study in [27] identified six morphological types, i.e., five types of projection neurons and one type of interneuron, with a number of subtypes. These types will be considered with respect to the position of their somata, their pattern of dendritic arborization and their axonal projections. The distribution and sizes of *H.Italicus* tectal cells are found in figure 2.5.

TO1 neurons: Their wide and large candelabrum-shaped dendritic trees arborize extensively and densely into layer 1 and sparsely in layers 3 and 4, so they are likely to receive retinal input predominantly from layer 1 RGC and to a lesser degree from layer 3 RGC. Their somata are situated in the superficial cellular layer 6 or in efferent layers 4 and 5. The axons descend bilaterally to the tegmentum and contralateral to the medulla (up to the 7th nerve which is mouth opening) and constitute the crossed tectobulbospinal tract [6].

TO2 neurons: Their large and wide dendritic trees are evenly distributed in layers 3 (dense) (primary dendrite) and layer 2 (secondary and tertiary dendrites)(wide) (RGC). Some cover up to one third of one tectal hemisphere in the mediolateral direction and extend along the border between layer 1 and and two for considerable distances. In cross sections the entire half of the tectum is covered by dendrites of one single neuron. Somata are located in the upper part of layer 6. Axons descend ipsilaterally to form a dense neuropil within the nu-

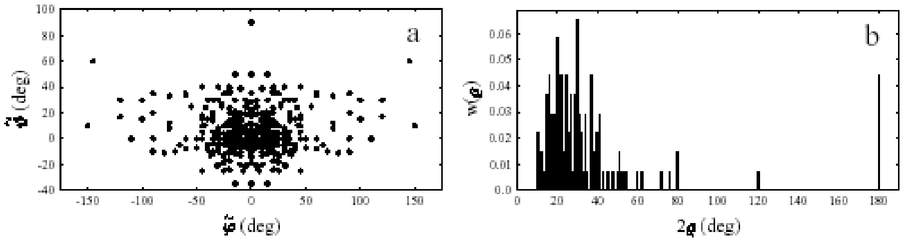

Figure 2.5: Properties of tectal neurons in *Hydromantes Italicus*. Distribution of receptive fields centers in the visual field (on the left) and Distribution of receptive field sizes. From [9].

cleus isthmi and usually descend also to the medulla (sparsely) and (constitute the lateral part of the uncrossed tectobulbospinal tract, to the 3rd spinal nerve). All neurons have axons that ascend to the ipsi- and contralateral pretectum and thalamus (2/3 are bilateral, 1/4 are ipsilateral projections) [6]. They are low in number.

TO3 neurons: Their flat and wide dendritic trees (midline and lateral edge, thick primary dendrite and thinner secondary dendrites) arborize primarily in layers 3(lower), 4 and 5. They predominantly process information coming from layer 3 RGC and from nonvisual afferents terminating in layers 4 and 5. A thick primary dendrite bends laterally within these layers. Somata are located in superficial or deep parts of cellular layer 6 or 8. With regard to axonal projections, three subgroups were identified: descending ipsilaterally within the medulla up to the 7th nerve) thus contributing to the uncrossed tectobulbospinal tract, ascending to the ipsi- or contralateral thalamus or both [6]. TO3 neurons are unevenly distributed in the tectum.

TO4 neurons: Their narrow dendritic trees are mainly confined in layers 3 and 2 (RGC) (also sparsely in layer 1). Somata of these rarely labelled neurons are situated in the deep cellular layer of the tectum. Axons descend ipsilaterally to the medulla oblongata and nucleus isthmi and other axons or axon collaterals ascend to the ipsilateral pretectum and thalamus [6].

TO5 neurons: Their small and narrow dendritic trees extend straight to fiber layers 1 and 2 or 1 and 3 [27]. Somata are situated in layer 6 and less often in layer 8. Axons only ascend to the ipsi- and contralateral thalamus and pretectum (they give rise to a distinct neuropil in the dorsal thalamus) and no axons were found projecting to the medulla [6]. They are evenly distributed from rostral to caudal tectum.

TO-IN neurons: Tectal interneurons receive no direct retinal input. Several subtypes were identified (6-7 out of 3 generic) [27]. They are at any depth and arborize in various layers. The diameter of the dendritic fields is smaller and no axon can be distinguished from the dendrites.

The projection neurons (except some TO4) were all excitatory first responses at short latencies followed by excitatory or inhibitory, interneurons showed inhibitory and/or excitatory at long latencies. It remains to be clarified in which way and to what degree the different types of efferent cells interact with each

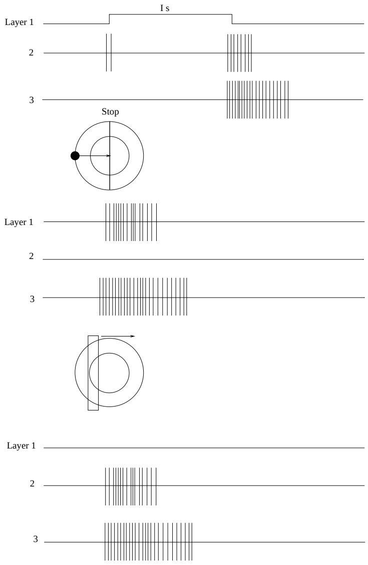

Figure 2.6: Responses of layer-1, layer-2, and layer-3 neurons in the optic tectum of *S.salamandra.* Stimuli are light on-off (upper), a small moving object stopping in the excitatory receptive field (in the middle), and a large vertical bar (lower) passing through the excitatory and inhibitory receptive field. From [26]

other. Multiple staining[2] between overlapping projection neurons and interneurons occurred. The combined neurons were arranged in columns (i.e., all were related to the same area in visual space). Figure 2.6 shows some responses of tectal neurons.

Number of Tectal Neurons

Total number of tectal cells in S.salamndra is 150,000 and 92,000 in *H.Italicus.* In *H.Italicus* 5000 from these cells are descending and ascending projection neurons (represent only 5% of the total number, the rest are innterneurons) and 3300 project to the medulla. Estimated numbers of projection neurons[3] in [6] are 660 TO1, 45 TO2, 950 TO3 and 25 TO4. TO5 present around 40% of all projecting neurons.

Tectal Neurons Afferents

The tectum receives afferents from different types of retinal ganglion cells and from other visual centers, e.g., pretectum, thalamus, and tegmentum, which themselves are targets of retinal afferents [6]. Neurons from tegmentum and medulla (also spinal cord) give rise to ascending fibers that extend in fiber layers 2 and 3 (retinal afferents) and into 4 (tectal efferent and non-visual afferents) [28]. Termination sites of ipsilateral and contralateral isthmic terminals are highly specific (see section 2.3.3).

---

[2] Probably du to coupling via gap junctions.

[3] These numbers vary in different studies.

Tectal Neurons Efferents

Axons of the optic tectum form the two tectobulbospinal pathways (i.e., crossed and uncrossed fiber tracts). They both extend to the medulla oblongata and spinalis, one-half to one-third of axons reach the level of the third spinal nerve [6]. The crossed tract is much broader and widespread than the uncrossed one. The significance of these difference is unknown [23]. 10% of projecting neurons (principally TO2 and TO4 neurons) terminate in the ipsilateral nucleus isthmi. The ascending pathways (i.e., to pretectum and thalamus) are constituted mostly by TO5 small- field neurons and by TO2 and TO3 widefield neurons. TO5 neurons could give rise to a retinotopic tectal projection to the thalamus.

Functional Assumptions

We can only speculate about the functional role of efferent pathways by considering the nature of their retinal input. T01 might be involved in object recognition (contrast and shape) also object localization based on the principle of coarse coding (Wiggers et al 95, Eurich et al.) [27]. TO2 and TO4 pathways are most probably involved in object recognition based on motion and movement pattern and TO3 process multisensory (i.e., somatosensory, auditory, vestibular) information and detection of large objects which could be enemies [27]. One should be cautious to ascribe a single function to different types of projecting neurons because all of them receive more than one type of retinal input and interact inside the tectum [27].

Descending pathways mediate different aspects of visual and visuomotor processing. The crossed tract may mediate information about location and shape of prey objects to premotor and motor centers and the lateral uncrossed tract about object movement [6]. TO2 and TO4 cells and the serotonin afferents may constitute an attentional system. The broad uncrossed tract certainly is involved in the integration of visual, somatosensory, and vestibular information. Visually, it may mediate information about movement of large objects and about changes in general illumination caused by such objects [6].

2.3.3 Nucleus Isthmi

The nucleus isthmi receives input mostly from TO2, TO4 and a few TO3 tectal cells and bilaterally projects back to the tectum [39]. Thus 4 representations of the visual field coexist and superimpose in the optic tectum (i.e., from direct contralateral and ipsilateral retinal, crossed and uncrossed isthmic afferents) [36]. The ipsilateral isthmic terminals extend through tectal layers 1-3, contralateral isthmic terminals are confined to layer 1 [34]. Isthmic afferents arrive to the tectum with a delay of 10-30ms with respect to retinal. The nucleus isthmi is retinotopically organized (see figure 2.3). Receptive field centers are all situated in the frontal 100°. Response properties, receptive field sizes, stimulus size and velocity preferences are very similar to those in the tectum. In the cases of binocular neurons (50%), the ipsilateral receptive fields are 35% smaller and completely surrounded by contralateral receptive one (their centers are displaced) [36].

As it receives input from and projects back to the tectum, the nucleus isthmi is considered as the main relay station between tectal hemispheres [36]. However the question of its specific function remains as it is well developed even in salamanders with massive direct ipsilateral retinal afferents. It is regarded to play an important role on depth perception based upon disparities between the left and the right eye. However the delay of 10-30ms between retinotectal projection and isthmotectal backprojection may considerably impair the accuracy of depth perception with respect to fast moving objects [36]. On the opposite, this delay could be used to calculate prey-movement trajectories in the visual field. The nucleus isthmi may also be involved in spatial-object selective attentional processes by providing a positive feedback to the tectum (i.e., spotlight effect) [34].

2.3.4 Pretectum

The pretectal area has been ascribed a role in *optokinetic nystagmus* (G. Manteuffel 1984, 1987; Làzàr et al. 1983), *figure-background discrimination* (G. Manteuffel 1985, 1986), *pupillary reflex* (Henning et al. 1991; Henning and Himstedt 1994), *fixation* (G. Manteuffel 1979), *phototaxis* (Himstedt and Manteuffel 1985), and particularly *prey-enemy distinction* [23].

Projection Patterns

The pretectum receives direct retinal input from both retinae and does not show stratified arborization as tectal neurons (i.e., arborizes homogenously) [20]. It projects in parallel to more than one target and in the study by Luksch et al. (1998) all labelled neurons were projecting neurons [23]. Axonal projections were divergent and widespread, which suggests that pretectal neurons are not part of a sequentially operating system, but have a modulatory role. A detailed information on pretectal projection targets can be found in Table 2.3.

Morphology and Response Properties

A classification of pretectal neurons on the basis of axonal termination patterns or dendritic arborization was not possible [23]. The labelled neurons were monopolar with a primary dendrite ramifying extensively-homogenously and multiply labelled neurons indicated an overlap of the dendritic trees [23]. Most pretectal neurons have large receptive fields (36-50°) and show a preference for square stimuli [26, Chapter 5]. Large receptive fields corroborate the idea that the pretectum is not primarily involved in prey recognition or guidance of feeding. Variations in latencies may indicate direct retinal input and indirect input [22]. Some of the studied neurons were direction-sensitive (i.e., neural activity is enhanced if movement in a specific direction is presented in the visual field and it is completely suppressed for the opposite direction) [28]. Two-thirds of the direction-sensitive neurons studied showed a sensitivity for temporonasal movement (i.e.,from the peripheral to the frontal part of the visual field, see figure 2.3, right). These neurons usually possessed large receptive fields with mean horizontal 82° and vertical 34° of the visual field. Their center was always in the contralateral visual field and they were sensitive to low velocities.

Pretectal Projections to Tectum

The exact nature of pretecto-tectal interaction is of special interest because of its specific function in prey-enemy distinction, background-discrimination (Buxbaum-Conradi and Ewert 1995; G. Manteuffel 1987) and object recognition (Grobstein 1987; Gruberg 1987; Roth 1987). However no subpopulations of pretectal neurons that might exclusively subserve one of these functions were found and most pretectal neurons had several axonal termination fields in various parts of the brain [23].

Especially Ewert model (1995) for prey-enemy distinction based on lesion data has been repeatedly questioned. This model assumes that the pretectum exerts an inhibitory influence on a particular type of tectal neuron with "gestalt recognition"[4] properties [23]. However, results of intracellular tracing studies do not support this hypothesis. The projection of pretectal cells to the optic tectum are bilateral with only sparse interactions and no precise wiring. No regular arborization pattern (bands and patches) could be observed [20]. This implies a modulatory role of the pretectum rather than a precisely wired inhibitory system [23].

According to [23] predominant diffuse projection to the ipsilateral tectum may be involved in the control of the optokinetic nystagmus, and contralateral efferents may be involved in the control of the pupillary light reflex. However they could not confirm Manteuffel's object-background discrimination model which predicts excitatory contralateral and inhibitory ipsilateral projections.

	Telencephalon	Diencephalon	Mesencephalon
Total	5 (22%)	21 (91%)	17 (74%)
Ipsilateral	2 (9%)	19 (83%)	15 (65%)
Contralateral	5 (22%)	10 (43%)	4 (17%)
	Optic Tectum	Medulla Oblongata	Spinal Cord
Total	11 (48%)	18 (78%)	7 (30%)
Ipsilateral	8 (35%)	16 (70%)	6 (26%)
Contralateral	5 (22%)	3 (13%)	1 (4%)

Table 2.3: Projection areas of completely labelled pretectal neurons. Absolute and relative numbers are given to indicate how many of the 23 labelled neurons projected to a given target on the ipsilateral or contralateral side of the brain, from [23].

2.3.5 Stimulation and Lesion Experiments

Stimulation or destruction of different parts of the brain is a way to put light on their functional behavior. When a part of the brain is ablated and subsequently the animal fails to perform certain tasks, there are good reasons to believe that this part of the brain is involved in performing these tasks. However these operations are with limited precision (i.e, destruction of one part can not be

---

[4] A typical perceptual experience in which the whole is understood as something more than the sum of the parts. Furthermore, this gestalt may be perceived before the parts comprising it.

done without destroying other parts) which yields contradictory data and it occurs often that the animal recovers from the deficiency within several week (remember that the brain tissue is plastic).

Various parts of the brain of *S.salamandra* were stimulated electrically using chronically implanted steel electrodes (Finkenstädt and Ewert, 83; in [26, Chapter 5]). By stimulating the **optic tectum** motor patterns for prey-catching behavior (i.e., orienting, approaching, snapping or biting) could be released. Stimulation of different positions within the tectum showed turning responses with various orientations that roughly corresponded to the *retinotopic map.* Stimulations with higher levels of electric current or focal application of strychnine or curare (Ingle,76) [4] to the surface of the optic tectum elicited exaggerated avoidance movements when an object passed through the corresponding region of the visual field. Electrical stimulation of **thalamus** and **pretectum** elicited avoidance behavior.

After ablation of the entire **optic tectum**, both visual prey-catching and predator avoidance behavior fail to occur to the objects in the affected monocular fields (Bechterev 1884 Ewert 68, Ingle 70) [4]. However the binocular field is spared as the whole contralateral eye projects onto one tectal hemisphere 2.3.2 (thus the binocular field is represented twice in the tectum). Local lesions produce scotomata (i.e., a total blindness for a small part of the field of view [40]) in the visual field (Sperry 45) [26], which is a result of the retinotopical representation of the tectum. Visual functions such as the optokinetic nystagmus 2.5 and barrier avoidance do not disappear (Ingle 73) [26, Chapter 6].

Ablation of the **nucleus isthmi** [4] is very similar to that obtained for tectal ablation, resulting in a scotoma in the monocular field of the affected side (Caine and Gruberg, 1985). Its lesion abolished response to threat stimuli in certain parts of the visual field, depending on the extent of the damage. Collett and Udin (1983) observed only occasional snapping at ghost objects.

Lesions of the **pretectum** facilitate feeding and abolish prey-predator discrimination [26]. Animals with unilateral lesions of pretectum responded with feeding toward moving objects of any size and configuration (respond to everything that moves including their own extremities and attack rather threatening stimuli) within the visual field contralateral to the lesioned brain region and escape behavior failed to occur. The size of the area in the visual field where feeding disinhibition occurred corresponded with size of the lesions [4]. The "worm-antiworm" discrimination was also strongly impaired and the receptive fields of some tectal cells increased from about 30 to 50 degrees (thalamo-pretectal (TP-phenomenon) known from anurans). Interestingly they return to "semi-normal" behavior after some weeks (Ingle 80, Ewert 83) [26, Chapter 6]. Manteuffel et al. (1983) reported an abolishment of the head optokinetic nystagmus 2.5 and a dilatation of the ipsilateral pupil after destruction of the pretectal neuropil (which did not occur after optic tectum lesions).

Ingle (1979) found that frogs with bilateral aspiration lesions of caudal **thalamus** where unable to avoid colision with a vertically striped barrier that partly surrounded the animal-demonstrating that the region is involved in obstacle negotiation. [4]. Lesions to rostrodorsal thalamus exhibited same symptoms as pretectal lesions but only the binocular field was affected [26]. Animals with ventral thalamus lesions showed no disinhibition with respect to feeding and exhibited abnormal body postures such as extreme body bending [26].

Unilateral lesions of a defined caudal tract in frog **medulla oblongata** do not produce any scotoma, however the animal always responds with a forward directed movement or a forward snapping(Kostyk and Grobstein 82, Grobstein and Massimo 86) [4]. After lesions in dorsal medulla junctions the animals make appropriate turns but advance incorrect distances and overshoot their prey. It can be concluded that different components of the stimulus position (eccentricity, elevation and distance) are *handled though different pathways* that can be disturbed independently [4].

Interestingly lesions of other parts of the brain can enhance a variety of behavioral responses such as aggressive behavior, ducking, creeping backward, raising the rostral trunk, or opening and closing the jaws.

2.4 Depth Perception

Main mechanisms for depth perception in salamanders are binocular triangulation and accommodation.

Salamanders accommodate during fixation on near prey (Werner,83) in [26]. However lens accommodation is a far too slow process (some salamander species possess a very small protractor lentis and is rather ineffective in moving the lens forward) and when the lentis is immobilized (deactivated with chemical substances), salamanders perform well. Thus binocular distance estimation is possible without accommodation.

On the other hand, binocularity is not necessary for good depth perception. Monocularization does not lead to any substantial impairment of depth perception and is quite common in species that show a high degree of aggressive behavior. (Luthard-Laimer,83) experimented on binocular animals, chronically monocular animals (one eye has been excised one year before) and reversibly monocularized salamanders (one eye covered with a tiny aluminium cap). Binocular animals snapped with a success rete of 40% , chronically monocularized animals were only slightly inferior with 36.5% and snapping success of reversibly monocularized salamanders was significantly lower with 26% [28].

With one eye covered *Hydromantes Italicus* shows a conspicuous approach behavior toward a prey. It takes a curved path to approach the prey and bends his body away of it toward the side of the seeing eye, compensating the bending by turning the head between 60° and 90°.

Tongue-projecting salamanders possess all the requirements for stereoscopic depth perception. The contralateral retinotectal projection from one eye and the ipsilateral from the other are in register. The two monocular receptive fields of binocular neurons exhibit zero disparities (horopter) with the maximum reach of tongue. Contralateral participation to binocularly driven neurons activity is up to 93%. A model for binocular depth perception based on tectal disparities is presented in [37].

2.5 Compensation for Visual Background and Head Movement

Self-motion produces a shift of the whole visual environment across the retinae and induces errors in localizing moving objects. Image and head stabilization are mediated by the *optokinetik* and *vestibucollic* reflexes [24]. The latter

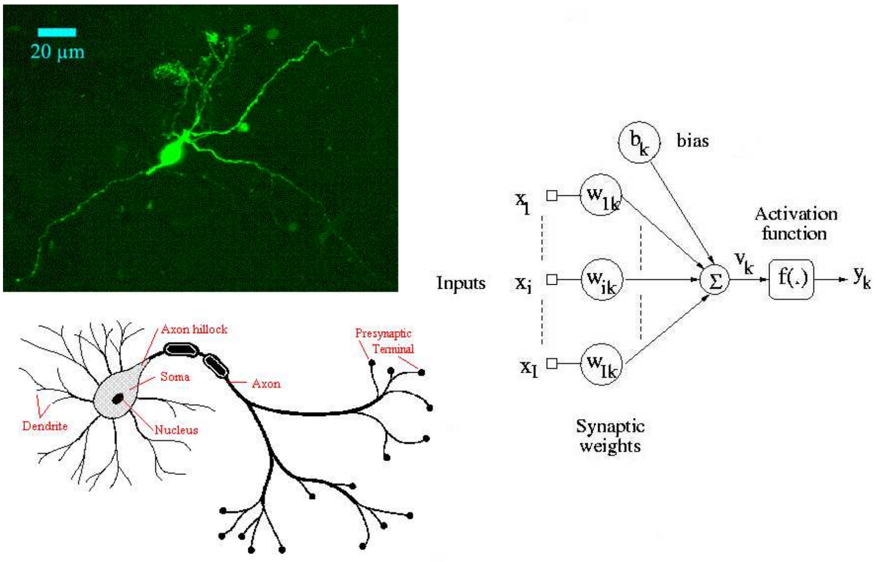

Figure 2.7: Analogy between the real and artificial neuron. Biocytin staining of a real neuron in the upper left corner, parts of a neuron in the lower left; and the artificial neuron.

compensates body undulations by antagonistic movements [24]. *Optokinetik Nystagmus* consists of a slow compensatory pursuit phase of the direction of stimulus movement, interrupted by occasionnal saccades in the opposite movements, which reset the head into more or less medial position [23]. During slow pursuit movement the head accelerates for a few seconds, until maximum velocity is reached. After a saccade there is again a build-up phase. These reflexes are able to compensate only 50-80% of the shift velocity in salamanders and the rest is directly computed in the optic tectum [24].

2.6 Neural Networks

The artificial neuron is a model motivated by analogy with the brain as the brain is capable of solving currently intractable complex problems 2.7. Artificial Neural Networks are particulary interesting because they perform massively parallel distributed computations and have the ability to learn and generalize [14].

The artificial neuron is defined by:

1. A set of *synapses* or connecting links, each of which is characterized by a *weight* or strength of its own. Specifically a signal x_j at the input of synapse j connected to neuron k is multiplied by the synaptic weight w_{kj}. Unlike a synapse in the brain, the synaptic weight of an artificial neuron may lay in a range that includes negative as well as positive values.

2. An *adder* for summing the input signals, weighted by the respective synapses

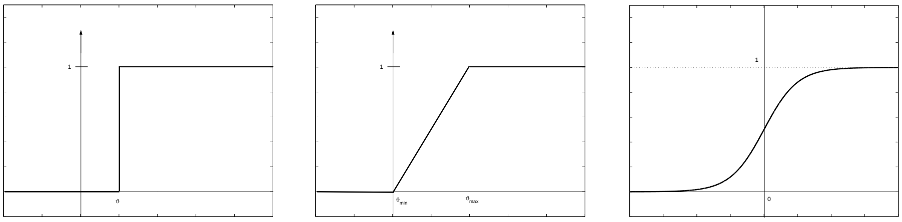

Figure 2.8: Different Activation Functions. From left to right. Binary function with threshold ϑ. Linear activation function. Hyperbolic activation function. From [12].

of the neuron.

3. An activation function for limiting the amplitude of the output of a neuron.
4. May also include an externally applied *bias*, denoted by b_k which has the effect of lowering or increasing the net input of the activation function.

In mathematical terms a neuron k is described by the following equations:

$$u_k = \sum_{j=1}^{m} w_{kj} x_j \tag{2.1}$$

and

$$y_k = \varphi(u_k + b_k) \tag{2.2}$$

where x_1,x_2, ...,x_m are the input signals (dendrites); w_{k1},w_{k2}, ...,w_{km} the synaptic weights of neuron k; b_k is the bias; $\varphi(.)$ is the activation function; and y_k is the output signal (axon).

The activation function, denoted by $\varphi()$ can be defined as binary, linear, hyperbolic or other (see figure 2.8).

2.6.1 Neural Maps Interaction

Several neural maps relating the animal to the space around it exist in the brain such as visual, somatosensory, auditive or motor (i.e., if we record the activity in a given region of the neural sensory surface, it will correspond to a given position in the visual field or skin)(see fig.2.9). The relation between different neural maps is far from simple. A particular point in the topographic map is not invariably linked to the the same locus in motor map, since different stimuli (e.g. prey or predator) located in the same part of the visual field may yield completely different responses [4]. The transformation from topographically to intensity coded maps and the transition from eye-centered topographical map to body-centered map represents another difficulty. We will investigate one possible transformation of visuoneural activity into motor patterns.

Figure 2.9: The amount of cortex that the brain devotes to different parts of the body is in direct proportion to their relative importance. In the motor cortex for example, more space is devoted to the fingers and lips than to the shoulder or elbow producing a sort of deformed map of the body. Such a map is known as homunculus. From [40].

Chapter 3

Previous Work

Several neural networks that account for specific tasks in visually guided behavior in salamanders have been realized, based upon the principle of *coarse coding.*

3.1 Coarse Coding

The high sensory resolution and the behavioral precision observed in localization experiments seems to be contradicted by the large receptive fields of the neurons involved (i.e. only small receptive field neurons are involved in object localization, whereas large receptive field neurons are responsible for large-scale movements and predator detection (Grüsser-Cornehls 1984; Gaillard 1985)) [8]. Tectal neurons in the tongue-projecting salamander *Hydromantes italicus* have a mean receptive field diameter of 41, with a minimum of 10° and a maximum near 360° (Wiggers et al. 1995).

The *coarse coding* mechanism developed by Eurich et al. (1997) suggests that it might be possible to calculate the resolution obtained by *population-coding* neurons, using mapping combinatorics of receptive fields. All neurons participate in the information coding (i.e., distributed information) and a non-firing neuron conveys as much information as a non-coding one [8]. It is shown that particularly large field neurons yield a high resolution, best resolution is achieved with 180° receptive field neurons [8]. However coarse coding has been considered with only one stimulus so far and it is likely that it suffers from *metamery* (i.e., convergence of information channels, can not discriminate between many objects because different objects yield the same perceptory activity).

3.2 Simulander I

Simulander I [7] is a feedforward neural network simulating the orientation movement of salamanders. The network was trained by means of an evolution strategy. It showed that accurate head orientation can be obtained despite a low number of tectal neurons (100) and large receptive fields. It is based upon the principle of *coarse coding* described in section 3.1. The information is distributed over the whole neuron layer and all neurons participate in the information processing. It is the cooperation of many neurons that leads to a high angular resolution.

The receptive field sizes and distribution are directly taken from experimental data (i.e., mean diameter of 41° and numerous 180° receptive fields, see figure and most receptive fields are situated in the binocular part of the visual field, see figure 2.5). The firing rates are adapted from electrophysiological experiments. They are a function of the stimulus angular size and stimulus angular velocity. However these values are not perceived by the salamander, but correspond to the obserever knowledge. The tectal neurons project onto 4 pools of interneurons and motoneurons governing four abstract muscles realizing the principle of antagonistic muscles. The projections to the neurons and interneurons are made to ressemble the crossed and uncrossed descending pathways. However not one tectal neuron type was found to project to both tracts simultaneously (see 2.3.2). The network was trained with a 0.6 randomly (randomly) moving prey with a mean Δvelocity of 0.5 cm/s or 20°/s (time steps of 0.2s). The success rate was of $86.3 \pm 0.3\%$, which is the generalization capability. Except for some positions it copes for motionless preys. It was also tested with larger angles as such patterns did not occur often during the training phase. It takes 5 seconds to orient the head toward a stimulus at 70°, which is rather slow. The removal of a tectal hemisphere accounts for investigations made in monocular salamanders, which was not considered when the network was constructed. The network does not take into account perceptional problems like figure-back-discrimination or prey-predator discrimination.

A set of different networks could generate similar performances and the large RF-s were important for successfully localizing the prey. The mapping was unstructured, no correlation could be found between weights and receptive fileld diameters or the position on the tectum, which does not instruct us the way how the network works.

3.3 Simulander II

The coarse coding mechanisms (see section 3.1) are applied to the specific task of tongue projecting in [9], which necessarily implies depth perception. Distance of prey, as evaluated by binocular neurons, is translated into commands for control of the projectile tongue. A discrimination of small regions of space is possible with an ensemble coding (see figure 3.1). A feedforward network was trained using an evolution strategy. The input layer consisted of 144 binocularly driven neurons, a layer of 12 interneurons and one motor neurons layer innervating 2 muscles. Each tectum neuron projects to 50% of both layers. The positions and sizes of the binocular neurons receptive fields are adopted from electrophysiological measurements in *Hydromantes Italicus*. However the simulation is confined to only central shots assuming the appropriate head position is a result of Simulander I network (described in section 3.2). However *bolitoglossine* salamanders are able to shoot their tongue laterally, sometimes combining lateral head movements. Simulander exhibits a protraction in all cases when the prey is within reach. It results in a success rate of 80% and 100 %. In the region immediately beyond the maximum protraction length (5cm) the performance is inaccurate. An object which is far away elicits reaction in many tectum neurons, this feature being an immediate consequence of the shape of the binocular fields

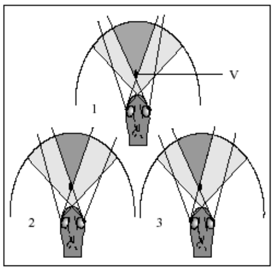

Figure 3.1: An example of the discrimination of a small region of space, V, with large binocular receptive fields (dark grey). V is characterized by the fact that it lies within receptive field 1 but not within receptive fields 2 and 3. The light grey shading indicates the binocular visual field. From [9].

and topology of the network. It predicts that the tongue overshoots if the prey is close.

3.4 Simulander III

The computer model Simulander III is a simple, biologically motivated neural network for the segmentation of a moving object from a visual scene [38]. It consists of an object selection model which employs scaled receptive field sizes, and a spotlight network which enhances the retinotectal transmission in a certain region by means of multiplicative synapses [38]. The selection criteria are largest angular width and largest angular velocity. The model yields possible explanations for the width distribution of the receptive fields of neurons of the tectum opticum, or for the range of velocities of objects for which Hydromantes italicus shows prey-capture behavior [38]. The double-dummy experience was simulated using this model (i.e., the animal has to choose one stimulus out of two identical, coherently moving prey-stimuli).

Chapter 4

Implemented Models

In this section we present the models developed within this project. We first introduce the neural networks implementation used in our simulation, followed by the descriptions of the theoretical models of the retina (photoreceptors and retinal ganglion cells), the optic tectum and pretectum, and the model for snapping behavior. As models are symmetrical, i.e., identical for the left and right sides of the salamander (side preferences are not significant in salamanders [29]), they will be presented for one side only.

4.1 Neural Networks Model

In order to faithfully reflect the biological mechanisms that occur inside the salamander's brain we naturally use neural networks circuitry (for a short introduction to neural networks please refer to section 2.6). Within the framework of this project we have developed a very easy to use interface for creating highly parameterized neural networks. This feature greatly facilitates the future integration of neural networks modelling the salamander's brain.

4.1.1 An Idealized Neuron Network

The neurons are **uniformly distributed** inside the network which results into a *grid* neuron layer (or a neuron *matrix*). We accord the same importance to the frontal and peripheral fields, thus losing the magnifying function (see figure 4.1). This has no significant impact on our results as it only exaggerates the peripheral resolution used in the orienting task (before gazing) task[1]). We also approximate the by using **square receptive fields** (rather than round or oval). These simplifications are performance motivated (i.e., calculation with matrices and square visual fields is less computationally expensive and closer to the computer representation). In the future it would be interesting to investigate the use of different densities throughout the visual field.

---

[1] Nature has optimized by reducing the number of neurons used.

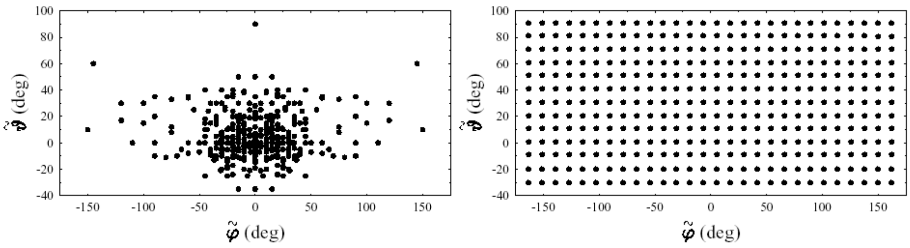

Figure 4.1: Distribution of the receptive field centers of *Hydromantes Italicus* tectal neurons [9]. Distribution of tectal neurons in our simulation.

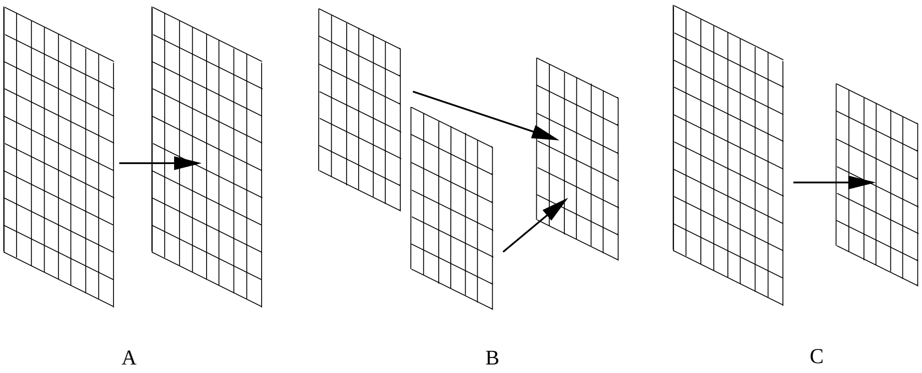

Figure 4.2: A. A feedforward architecture. B. Layer that compares temporally different signals. C. A reduction feature between two layers, several neurons from the first layer project onto one neuron in the second.

4.1.2 Neural Networks Implementation

When leaving aside some particular recurrent neural signals, visual brain processing is basically a top-to-bottom processing in the sense that the photoreceptors pass information onto the retinal cells which process the visual information and transfer it to the tectum cells which again project onto the motor neurons. Therefore we use **feedforward architecture** networks (see figure 4.2, A). "Time-dependant" networks (i.e., computing the difference between an immediate and a delayed signal) take two layers as input (see figure 4.2, B).

We also apply a **reduction** feature from one layer to another (see figure 4.2, C). These reductions occur frequently in the brain. *Hydromantes Italicus* for example has about 57.900 photorecetors, 46.400 retinal neurons [26, Chapter 3], 5000 projecting tectum neurons and only few motoneurons at the level of the brain stem. The processed information is reduced as it proceeds toward the output. One should be careful to preserve the correspondence between the layers (i.e., locally near neurons in the first layer should project to locally near neurons in the second layer).

A first implementation of the reduction feature was using a *reduction ratio.* The new network size equaled the *input network size/reduction ratio* and newly

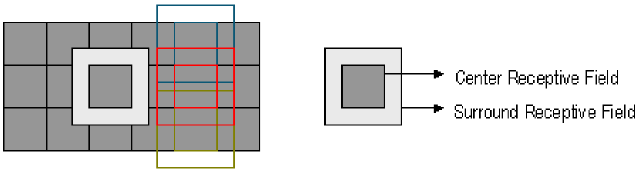

Figure 4.3: The center receptive fields of the neurons cover completely the network area. The size of the *analyze box* (in light grey) defines the degree of overlap.

created neurons were automatically organized to perfectly fit the whole receptive field area (i.e., the area covered by the input network). As in literature all neurons are defined by their center and surround receptive fields, we changed the neural networks specification to a more appropriate one. All one needs to specify are the sizes of the center and surround receptive fields (in degrees of the visual field). On the basis of the center surround field the program calculates the network size. Horizontal and vertical dimensions are chosen such that the center receptive fields cover the whole input network, when disposed regularly (see figure 4.3). This defines the neural network resolution. The surround receptive fields represent the **overlap**. It is used to calculate the size of the analyze box (in light grey in figure 4.3), which defines the actual mapping between the input network neurons projections and the newly created neurons. One input neuron may project onto several neurons. This enables us to explore and use the redundancy feature of neural networks, which is proven to be exist in the retina and suspected to present in the optic tectum. The details of the implementation will not be presented.

Subsequently the neuron network parameters need to be specified, i.e., the weights matrix, the activation function and the minimal and maximal thresholds (i.e., limiting values to avoid activation levels potentially dangerous for the salamander), introduced in section 2.6. The neurons are identical throughout the network for the sake of simplifying the initialization phase. It is noteworthy mentioning that linear filtering kernels [11]) used in traditional image processing are implementable in no time on the neural networks previously described.

New neural networks are implementable in a highly *parameterizable*, *automated* and *easy to use* way. Once the network is initialized, a processing and a displaying function may be called anywhere in the program. The **visualization function** enables you to display the "real-time" network activity at any time, which is an indispensable comprehension and debugging tool.

4.2 Retina Model

In order to implement a complete sensing-to-acting loop within the environment, we modelled the principal retinal components, i.e., the photoreceptors and the three types of retinal ganglion cells identified in salamanders.

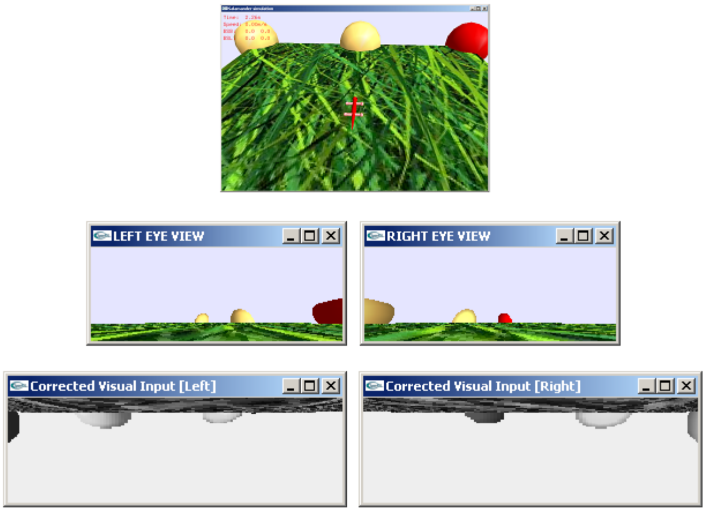

Figure 4.4: From top to bottom. Image of the Salamander World. What the salamander sees (all spheres are present in both eyes because of the large binocular field, notice the position of the red sphere). Spherical correction of the OpenGl extracted views (the spheres are no more distorted, as in the above image).

4.2.1 Photoreceptors

To simulate the retina *photoreceptors* we used functions provided by OpenGl (i.e., a low-level high performance 2D/3D graphics library specification). Virtual cameras were placed on the salamander's eyes and given an orientation they extracted a view inherent to OpenGl. This gave us images of what the salamander would see from his both eyes (see intermediate pictures in figure 4.4).

The eyes of the salamander are fixed in the head and do not allow eye movements. We approximated them by spheres with the node of dioptric apparatus in the center. The view extracted by OpenGl is a view projected on a plane. In order to be more realistic we project it again on a **spherical** surface, which corrects the OpenGl distortions (compare second and third line of figure 4.4). Because the visual input is projected through the retina node the retina image is inverted (see figure 4.4).

On visual fields

Different species have different visual field sizes (see Table 4.1) and this can influence the effectiveness of their vision. We wanted to be able to model any size of visual field in order to measure the effect it might have on the feeding strategy There seems to be a correlation between feeding strategy and amount of developed vision system, as species with well developed eyes feed using "ambush" strategy and the others use "hunter" techniques (see section 2.2.1 for more details). For the visual parameters of the simulated salamander we inspired ourselves from *Hydromantes Italicus* who has a rather developed vision, large horizontal and binocular visual fields (300° and 90° respectively; the boundary of 45° of binocular field on each side is to our opinion strongly correlated with the capacity of *bolitoglossine* salamanders to shoot their tongue laterally up to 45°). OpenGl did not make it possible to use so large horizontal fields as the image generated was not interpretable. Therefore we limited the horizontal field to 200° which is also the value used in [17]). A summary of used values can be found in table 4.1.

	Horizontal	Binocular	Vertical below horizon	Vertical above horizon
H. italicus	300°	90°	34°	60°
B. attenuatus	130°	70°	35°	45°
Simulation	200°	90°	30°	60°

Table 4.1: Areas of visual fields covered by the receptive fields centers in two salamander species and visual fields used in the simulation.

Color

Color-sensitive photoreceptors are easy to model in OpenGl by extracting the *RGB-values* of an image. In an early stage we simulated a low-illumination rod[2] by simply amplifying the signal. We used *grey-valued* views of the salamander world as we were not interested in color contribution to vision in salamanders.

4.2.2 Retinal Ganglion Cells

Retinal ganglion cells response is the visual information as passed on to the brain, more specifically to the optic tectum. According to [15] spatial summation of type 2 and 3 retinal ganglion cells and lateral tectal inhibition suffice to explain some of the tectal cells response properties. In the perspective of implementing a complete loop with the environment, we estimated important to simulate this retinal layer. The number of retina ganglion cells can range from 26.000 to 52.000 (depending on the species). In our simulation the number of retinal cells used is flexible so we can study how the visual acuity affects visually guided behavior. Three retina ganglion cells types have been identified in S.salamandra [26].

Type 1 Retinal Ganglion Cells

Retinal Ganglion Cells of type 1 are neurons with small-size excitatory receptive fields (2-3°) and strong inhibitory surround (12-16°), and no response to change in diffuse light. They give rise to a fine-grained representation of the visual field and are believed to be involved in local contrast calculation (i.e., edge detectors) (see table 2.2). They are mainly used by TO1 neuron which projects to the contralateral tectobulbospinal pathway, which means that they activate contralateral muscles and trigger movements toward the opposite side of the stimulus. Thus to our opinion they may be involved in obstacle avoidance.

---

[2] A photoreceptor specialized for night vision, 10^4 times more sensitive than cones (saturates by daylight) [40].

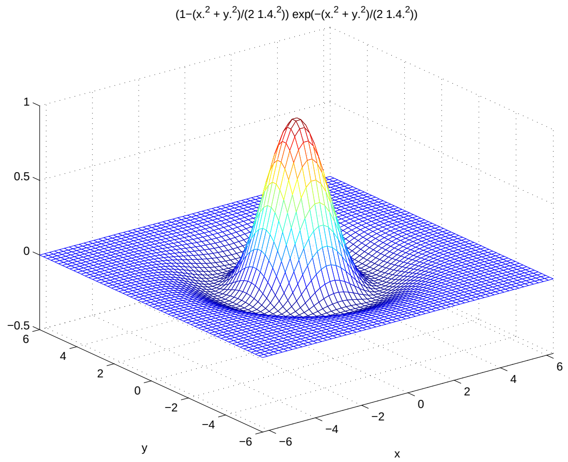

Figure 4.5: The Lapalacian of Gaussian filter kernel. Represents an excitatory center and inhibitory surround receptive field.

A computer vision strategy for detecting edges and sharp changes in brightness is the *Laplacian of Gaussian* filter (see figure 4.5) [11]. It is also confirmed that the receptive field of a larval tiger salamander has this ”Mexican Hat” profile [2]. The Laplacian (i.e., second derivative) of a function in 2D is defined as:

$$(\nabla^2 f)(x, y) = \frac{\partial f}{\partial x^2} + \frac{\partial f}{\partial y^2} \tag{4.1}$$

As difference estimates are sensitive to noise a smoothing function should be applied first [11]. So we convolve the image with the derivative (i.e., *Laplacian*) of a *Gaussian* smoothing kernel:

$$LoG = -[1 - \frac{x^2 + y^2}{2\sigma^2}]e^{-\frac{x^2+y^2}{2\sigma^2}} \tag{4.2}$$

where x and y are the pixel positions and σ is the standard deviation. We assigned the weights of the RGC1 neuron using a discrete version of this function. The result with different receptive field sizes can be observed in figure 4.6. RGC1 are not sensitive to change in diffuse light which implies that integrated weights have to be equal to zero (i.e., when all dendrites are equally excited they do not elicit any neural activity). We can make the cell sensitive to on-off changes in diffuse light by changing the value of the weights integral.

Type 2 Retinal Ganglion Cells

Retinal Ganglion Cells of type 2 respond only to moving objects. Most techniques for dynamic scene analysis are based on the detection of change (any perceptible motion results in some change in the sequence of scene frames) [19]. The most obvious method for detecting change is to directly compare the corresponding pixels of the two frames to determine whether they are the same.

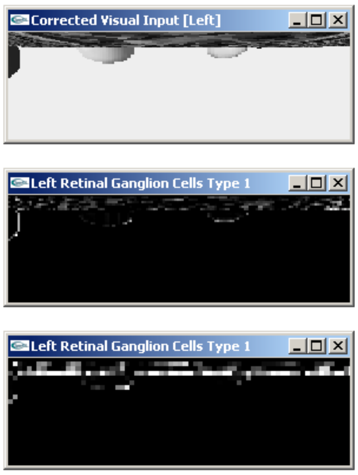

Figure 4.6: The response of retinal ganglion cell 1 network. From top to bottom. Photoreceptors input. Retinal ganglion cell with 1° ERF and 11° IRF. Salamander retinal ganglion cell with 2° ERF and 16° IRF. Standard deviation fixed to 1.4.

Difference functions make sense in biology. Two pathways with different delays processing the same information give rise to a double representation (i.e., the same information at different times).

A linear difference picture $f_{dif}(x, y)$ between frames $f(x, y, j)$ and $f(x, y, k)$ is obtained by:

$$f_{dif}(x, y) = \begin{cases} |f(x, y, j) - f(x, y, k)| - \tau & \text{if } |f(x, y, j) - f(x, y, k)| > \tau \\ 0 & \text{otherwise} \end{cases} \tag{4.3}$$

where τ is a threshold, k and j are moments in time and x and y are the pixel positions in the frame. We have chosen a linear function (instead of binary) in order to obtain contrast sensitive neurons. The absolute value makes sense, since retinal ganglion cells of type 2 respond to both on and off changes (see 2.6). k-j corresponds to one time step in the program. The threshold τ has been fixed to 0.25 with respect to the minimal contrast sensitivity for retinal ganglion cell 2 (see Table 2.2). The weights are equal throughout the receptive field in order to give account of the light intensity of an area without giving greater importance to particular points. There is also evidence that retinal weights are flat (i.e., have constant synaptic fields), since the activity sharply increases when the stimulus enters the receptive field [38].

According to this model the response of the retinal ganglion cell is the variation of light intensity in its receptive filed. The model is however not perfect as it responds to all self-induced movements (i.e., when the subject moves all stationery objects appear in motion). Ideally it should be coupled with another mechanism. It is extremely difficult to extrapolate self-induced movements from a scene. It is not possible to simply compare the position of an object and its self-induced position, as objects at different distances move with different velocities.

Type 3 Retinal Ganglion Cells

Our retinal ganglion cells of type 3 simply sum up the overall luminosity in their large receptive field. They have constant weights. This is consistent with data found on RGC 3.

4.3 Optic Tectum Model

The primary motivation for the project was to implement a simple model of the salamander optic tectum inside a closed loop with the environment as a solution to the amphibian visuomotor coordination problem. The idea was to construct a structured-mapping summing neural network proposed by Ijspeert, that would govern the neck and body muscles of the already existing neuromechanical model of the salamander [17]. The model was trained for the specific tasks of orienting and gaze stabilization.

The addressed question was to see to what extent this model could explain biological observations. Besides the mere task of perceiving its limits, the objective was to gain more understanding on how the model works, to explore and yield a representation of its parameter space. We expected that the model would to some extent account for object-background discrimination (see section 2.5) or at least make the difference between a large distant object and a small close one, having the same apparent angular size. These two objects stimulate the tectum in a very different way (see figure 4.14).

In section 5 we present results about the robustness of the model, graphs and interpretation of the parameter space, object-background discrimination results, the relation between number of neurons and resolution and how the use of overlapping receptive fields affects the model. We also account for different behaviors that were not considered while constructing the model but can be explained by it.

Biological Inspirations

We principally inspired ourselves from the fact that a topographical representation of the retina exists in the optic tectum (see section 2.3.2). Stimulation of different positions within the tectum showed turning responses with various orientations that roughly corresponded to this *retinotopic map* (section 2.3.5). The second motivation was the small number of synapses involved in visoumotor coordination (i.e., the retina passes visual information to the tectum which is directly connected to the brainstem motor centers via the medulla oblongata pathways). Therefore resolving the nature of tecto-spinal interaction would provide a solution for the visuomotor coordination problem.

The tectum (falsely called optic) integrates multimodal perception, such as olfactive, somatosensory or vestibular. We have concentrated our efforts on visual information processing only, because of the abundance of data on the subject. We also constrained ourselves to reproducing the terrestrial feeding behavior only.

The model is *intensity*-coded in the sense that it attributes different strengths to tectal neurons along the rostro-caudal axis (see figure 4.9). Thus the neuron

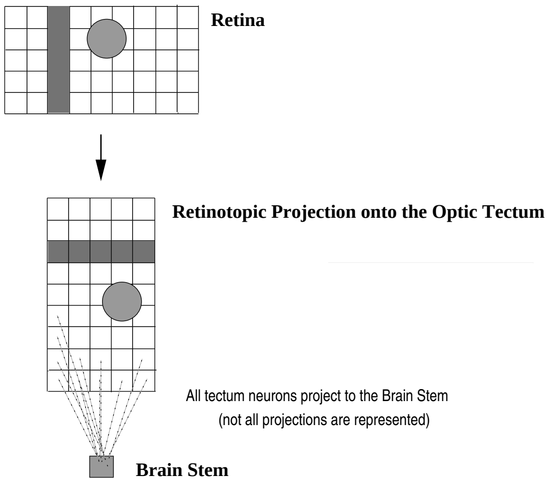

Figure 4.7: Objects with same eccentricity in the visual field are projected to the same line in the optic tectum. They have identical strengths when projected to the Brain Stem as they induce the same turning angle. Tectal neurons weights increase with the rostro-caudal axis. Only the left tectal hemisphere is represented.

response reflects the stimulus eccentricity (i.e., horizontal position relative to the eye). It is obvious that laterally situated stimulus should provoke a higher motoneuron activity in order to trigger larger orienting movements (see figure 4.7). It was challenging to search whether this particular mapping could work out as transcription mechanism between the eye-centered topographic map in the tectum and the body-centered intensity-coded motor map (see section 2.6.1).

We also use a *locally-coded* network in the sense that we divide the sensory field into cells and attribute the obtained receptive fields to single neurons (consistent with the retinotopical projection). The advantage of locally coding is that it does not suffer from *metamery* (i.e., convergence of the information channels, inability to discriminate between many objects because they yield the same perception activity). The main drawback is the important number of neurons involved. However this does not seem to be case here (see section 4.3). Subsequently large receptive field sizes were considered with respect to data on tectal field sizes (see figure 2.5). The effect of partly overlapping receptive fields was also studied.

Description of the model

We believe that TO4 cells are involved in object localization since they project to the nucleus isthmi 2.3.3 and arborize predominantly in layer 2 (motion-sensitive retinal ganglion cells). To our opinion the data on their low number is inconsistent with the narrow size of their dendritic fields. This is probably du to the methodology used (i.e., biocytin staining), which preferentially labels neurons in the superficial layers. Motion is a necessary prerequisite for a stimulus to be considered as prey 2.2.3. In our model the tectal cell response is similar to that

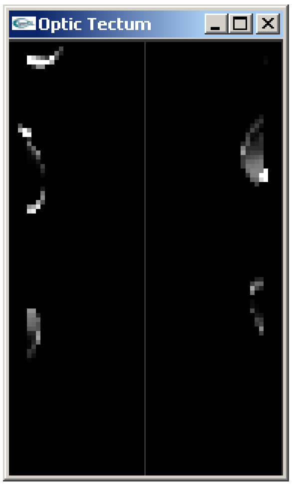

Figure 4.8: Tectal activity with moving spheres on the horizon. Retinotopic inversion was respected.

of the retinal ganglion cell as we do not integrate information from different sensory perceptions. The information conveyed by the tectal cell is a reduced version of RGC2 response (tectal cells are less numerous than retinal ganglion cells). An example of tectal activity with a simple visual input is shown on figure 4.8, the inverted retinotopy (see also figure 2.3) has been taken into account.

The tectal neurons' output is simply summed at the level of the brainstem. The tectal cell response is weighted using a linear function. The motoneuron activation function is as following:

$$f_M = \sum_i \sum_j \omega(\theta_i) x_{ij} \tag{4.4}$$

where i and j are the horizontal and vertical positions of the neuron in the tectal layer x. $\omega(.)$ is the weights function computed using:

$$\omega(\theta) = \alpha\theta + \beta \tag{4.5}$$

where α and β are parameters, and θ_i is the the horizontal angular distance of the tectum neurons (see figure 4.9).

Adding ipsilateral retinal input

Tongue projecting salamanders (*H.Italicus*, *bolitoglossine*..) are capable of precise depth estimation based on retinal disparity (see section 2.4). A fast comparison between the left and right visual cues is possible as they receive substantial ipsilateral input from the retinal ganglion cells in addition to the contralateral usual one. Additional ipsilateral retinal afferents make sense only in the binocular visual field (i.e., visual field seen by both eyes). The preceding model was modified to take into account both contralateral and ipsilateral retinal inputs:

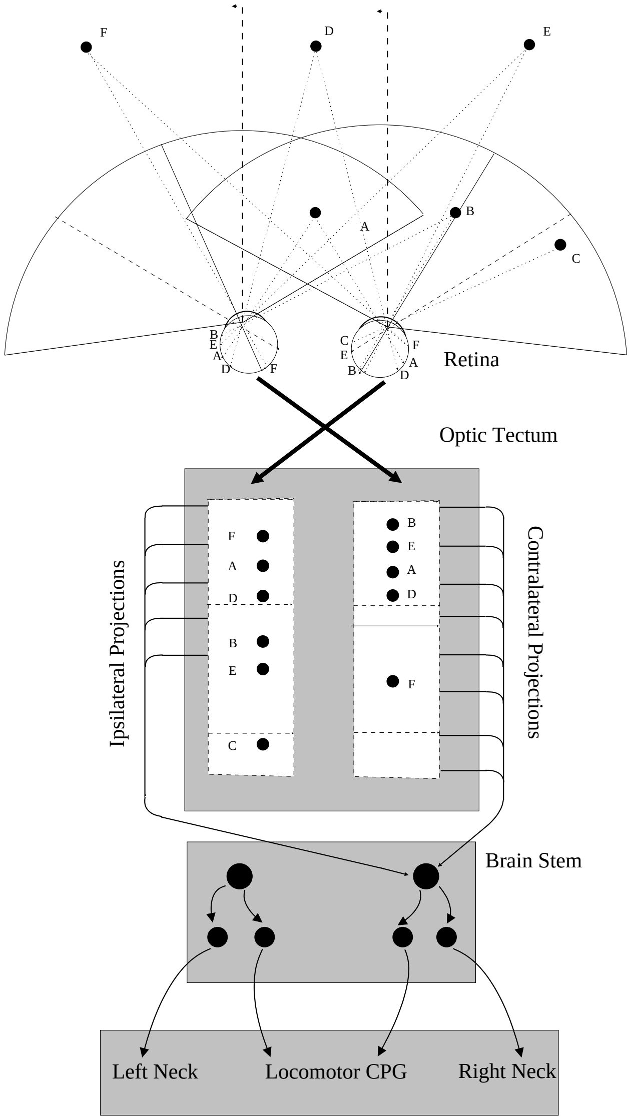

Figure 4.9: Mapping of the tectum projections to the brainstem. It also shows the representation of several stimuli in the tectum, which depends on the stimulus eccentricity. All points have identical elevation in the visual field as they are vertically aligned in the tectum. Normally the contralateral and ipsilateral representation of the visual field are projected simultaneously onto the same tectal hemisphere. However we wanted to avoid having double representations of the same visual input in our simulation, so we simplify by taking the ipsilateral projection from the other tectal hemisphere.

$$f_M = \sum_i \sum_j \omega^c(\theta_i) x_{ij} + \sum_i \sum_j \omega^i(\theta_i) y_{ij} \tag{4.6}$$

where x represents the tectal hemisphere which is on the same side of the motoneuron (with contralateral visual input) and y is the tectal layer on the opposite side (see figure 4.9). i and j are the horizontal and vertical positions of the neuron in the tectal layer and $\omega^c(.)$ and $\omega^i(.)$ are the respective weights functions.

$$\omega^c(\theta) = \alpha^c \theta + \beta^c \tag{4.7}$$

$$\omega^i(\theta) = \alpha^i \theta + \beta^i \tag{4.8}$$

where α^c, β^c, α^i, β^i are parameters and θ is the horizontal angular distance of the tectum neurons .

The ipsilateral and contralateral α and β were assigned through an extensive search of the parameter space. The fitness function was the error between the real stimulus angle (relative to the salamander body) and the salamander head angle resulted from the activation of the salamander motoneurons[3].

Improved model

The previous models work well for one type of stimulus. However if stimulus size is increased, more tectal cells will be stimulated thus augmenting the motoneuron activity. This will trigger larger orienting angles even though the stimulus has not changed place. Therefore there is a need to *normalize* the signal sent to the motoneuron. This procedure is biologically plausible. Tectal cells such as TO2 and TO3 have large receptive fields covering up to two thirds and more of the tectal hemisphere. There is also a peak of 180° tectal receptive fields of H.Italicus tectal neurons (see figure 2.5). We believe that these cells realize overall-calculations, such as summing tectal activity or calculating global movements direction. Connected via multiplicative synapses they could modulate signals produced by other neurons. We normalize the motoneuron activity in the following way:

$$f_M = \frac{\sum_i \sum_j \omega^c(\theta_i) x^c_{ij} + \sum_i \sum_j \omega^i(\theta_i) x^i_{ij}}{\sum_i \sum_j x^c_{ij} + \sum_i \sum_j x^i_{ij}} \tag{4.9}$$

where x represents the tectal hemisphere which is on the same side of the motoneuron (with contralateral visual input) and y is the tectal layer on the opposite side (see figure 4.9), i and j are the horizontal and vertical positions of the neuron in the tectal layer and $\omega^c()$ and $\omega^i()$ are the respective weights functions (as described by equations 4.7 and 4.8). We actually divide the summed weighted tectal activity by the overall tectal activity.

Number of Neurons

The following reasoning can be found in [9]: assuming the visual resolution of 0.57° (the salamander is able to localize a 0.05-cm sized prey at a distance of

---

[3] The locomotor circuit supports only horizontal movements of the head.

5 cm) 162 000 neurons would be needed to cover the whole visual field (with a locally-coded network).

However one should not confuse visual acuity of the animal and orienting head precision. The accuracy of prey localization in tongue projecting *H.Italicus* is about 3° (and not 0.57°) [38]. The size of the tongue pad probably compensates for this loss. *S.salamandra* is even less precise with a success rate of 39% [26]. This considerably changes the picture previously exposed. To cover the binocular field (90°x90°) of one tectal hemisphere (the majority of neurons are situated in the binocular field as is shown on figure 4.1) only 900 neurons would suffice to yield a resolution of 3°. This is much closer to the real number of descending tectal projections presented insection 2.3.2 than the number presented in [9]. To our opinion the visual acuity does not depend on the tectal cells resolution, but on retinal ganglion cells only. Our model will be tested to see if it responds to such small preys as 0.05 at 5cm despite the lower localization precision.

4.4 Brain Stem Model

The brain stem contains the premotor and motor neural centers. In our model the visual system output (equation 4.9) determines the tonic drive applied to the locomotor circuit (developed by Ijspeert), which activates the salamander CPG (i.e.,central pattern generator). During head orientation and gaze stabilization we stimulate the two neck muscles[4] using the motoneuron activation function described by equation 4.9. When approaching body muscles are contracted as well using an appropriately chosen tonic drive. Motoneuron antagonism was already inherent to the model, as turning movements are triggered by asymmetric input. The motoneurons accept negative weights which represent turns in the opposite direction (i.e., movements to the same side as the motoneuron). We easily rectified this little incongruity. There is also a simple feedback loop at the motoneuron level. The stimulus position in the visual field (as it is perceived by the salamander) is relative to the salamander's head position. Therefore every turning movement generated should be added upon the preceding.

4.5 Pretectum Model

We were particularly interested in modelling both prey and predator (i.e., feeding and escape) behavior .

A simple prey-predator discrimination model

When a dark moving object exceeds a certain size it always elicits escape behavior [26]. Beside detecting dark and large moving objects, pretectal cells are also direction-sensitive, especially in the temporo-nasal direction (i.e., from central to peripheral visual field, see left figure 2.3) [24]. Therefore the animal is alerted only for temporo-nasal direction movements which correspond to approaching objects. This mechanism also prevents false alerts. For example, the image shift of the environment during a forward movement could produce dimming effects.

---

[4] Left and right, each one inducing movements to the opposite side.

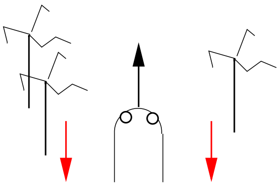

Figure 4.10: A forward movement of the salamander will produce a naso-temporal shift of the environment image.

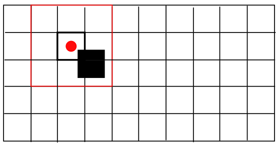

Figure 4.11: The neuron with dark black borders can not detect the large object in its receptive field, as only a small part is detected. The large neuron (in red) will infallibly detect any object of the same size.

As the shift occurs in the naso-temporal direction (see figure 4.11), the animal is not alerted. So the response to a pretectal cell would be the integrated response of a dimming detector neuron, a motion-sensitive neuron and direction-sensitive neuron:

f_P = large dark object * movement * temporonasal direction

Based upon lesion effects we know that the pretectum is involved in predator recognition and triggers escape behavior (see section 2.3.5). If the pretectum is abolished no escape behavior can be elicited and the animal snaps at everything that moves, even at its own extremities and threatening stimuli. Thus we believe that the tectum responds to all sizes of moving stimulus in the visual field (i.e., also predator-like sizes). A moving object larger than the receptive field of a motion-sensitive tectal cell activates the neuron to the same amount as moving objects with exactly the same size (as they both cover the whole receptive field). Thus to our opinion prey-predator discrimination, which is based upon the stimulus size, can not occur in the tectum. A large ”predator” stimulus (i.e., larger than a specific size) that appears in the visual field, is instead detected by the pretectum, and the pretectal signals override the tectal signals inducing escape behavior in the opposite direction. On the other hand, when the tectum is destroyed escape behavior fails to occur [26] and [4]. This indicates that pretectal activity somehow depends on the tectal activity.

Detector for large moving objects

As we know, retinal ganglion cells of type 3 respond to dark and large objects in the visual field (see 2.6). Moreover their size roughly corresponds to stimulus size that inevitably elicit escape behavior (16-20°). However if the object is not centered within the receptive field, it will be not detected (see the neuron with a red dot in the center, in figure 4.10). Only a neuron with a larger receptive field (the neuron with red contour in figure 4.10) can infallibly account for large objects in the environment. In our model a pretectal neuron exists for every RGC 3 neuron and sums its response with those of its neighboring cells. This model predicts that pretectal neurons RFs need to be three times larger than RGC 3 RFs, and this indeed is the case (i.e., 30-50° and 10-20° in salamanders). In our model pretectal neurons respond to objects with large angular size (not absolute)[5]. In *S.salamandra* this might also be the case. Depth perception is assumed to depend on the isthmo-tectal pathway which has a considerable delay of 30ms (see section 2.3.3), while escape behavior should be immediately released. Moreover *S.salamandra* often snaps at prey that are too large to be swallowed and its snapping success rate is only 40% [3] and [26], this attests a rather inaccurate depth perception.

To perceive the movement of large objects, we use the mechanism used in motion-sensitive retinal ganglion cells 4.2.2 (i.e., we compare the immediate and anterior responses of the pretectal dimming detector neuron described above). According to [22] variations in latencies found in pretectal cells may indicate simultaneous direct retinal and indirect retinal input. We know that the pretectum receives direct retinal afferents, and we also know that the retinal ganglion cells of type 2 and 3 that arrive in the tectum develop collaterals in thalamus and pretectum (see section 2.3.1). Therefore we assume that the indirect retinal input in the pretectum, needed to detect movement, arrives from the tectum. This could explain why in animals with tectum lesion escape behavior (normally attributed to the pretectum) is impaired.

A direction-selective neuron

The model for direction-sensitive neurons that can be found in literature is uncomplete. It is an early model that only contains guiding lines, and we do not know if it is really implementable. Therefore we came up with a very simple model of a neuron that accounts for directionally-specific global movements in the receptive field.

Our model is based upon separating the *ON and OFF channels* of the visual input. An OFF change accounts for a dark object that appears on a bright background and an ON change occurs where the dark object has dissapeared. OFF changes have negative values and ON changes are positive. Parts in which a dark object has appeared will have negative contribution in the receptive field and the trailing edge of the object will contribute positively (see figure 4.12). If the neuron weights are chosen to increase along a certain direction inside the receptive field, the neuron's activity will be enhanced when the object moves in the preffered direction and completely suppressed in the opposite direction. The on and off channels are separated with a difference function with no absolute value:

$$f_{dif}(x,y) = f(x,y,j) - f(x,y,k) \tag{4.10}$$

This model works only for dark moving objects. The change in light intensity du to an appearing dark object, can also be interpreted as the departure of

---

[5] There is evidence that the tectal cell response is sensitive to angular and not absolute size. We do not know if the same is true for pretectal cells.

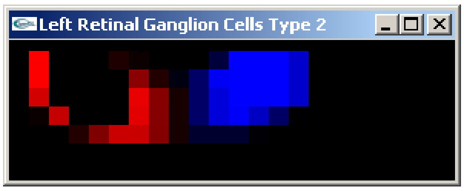

Figure 4.12: In blue OFF changes, in red ON changes. The object moves from left to right.

an object brighter than the background. The same seems to be the case in amphibians. *S.salamandra* does not seem to possess ON-units (i.e., stimulated with light on), (see figure 2.6). The toad Bufo Bufo fixates and snaps at leading edges of long black horizontal bars on white background and at the trailing edge of white horizontal bars on black background (Burghagen and Ewert, 1982) [38].

The response to many stimuli moving in different directions will sum all the contributions. Thus it will account for the faster or larger moving stimulus. The model does works for any direction.

A delay neuron

After a "predator" stimulus has released escape reaction, the animal flees in the opposite direction. In a few moments the predator gets out of sight and the pretectal cell is no more stimulated. However, pretectal stimulation of motoneurons should last a long time after the salamander has encountered a predator stimulus, at least until danger is away (i.e., in a way the salamander should remember it has seen a predator). In [24] a group of pretectal neurons in *S.salamandra* that were active after stimulating the pretectum is reported. Therefore we have introduced a neuron that prolongs the pretectal activity.

4.6 Snapping Model

A possible snapping model was investigated in order to give the salamander a restrained depth estimation capacity. For this task the salamander was given a tongue (see figure 4.13).

Tongue mechanism

Four biologically inspired muscles control the tongue protraction length and horizontal direction[6]: a tongue protractor (SAR, muscle subarcualis rectus), a tongue retractor (RCP, muscle rectus cervicis profundus); the shooting direction is controlled by the interaction of two types of muscles, the suprapeduncularis (SP) and the geniohyoideus lateralis (GHL) [5] and [26]. Unequal contraction of these muscles leads to lateral deviation of the cylinder (SP) projectile. Tongue muscles are not activated in a stereotyped pattern, but the protraction length and time are modulated by the stimulus distance [5]. Therefore protraction and retraction times in our simulation are also a function of the stimulus distance.

---

[6] The model could easily be extended to the vertical direction.

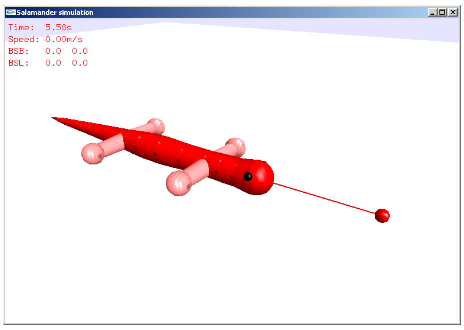

```
Time:  5.58s
Speed: 0.00m/s
BSB:   0.0  0.0
BSL:   0.0  0.0
```

Figure 4.13: The salamander has been given a tongue.

First the protractor and direction muscles are activated, followed by the retractor. We had to use a long retraction time because the salamander snapped at its own tongue continuously, interpreting it as a prey stimulus.

Distance Maps

A first attempt of constructing a distance-dependant perception of the visual scene was using a stereopsis algorithm. The disparity (i.e., displacement between the locations of an object in the left and right eye views) is sufficient to produce precise depth estimations. However traditional stereopsis algorithms ([19] and [11]) are iterative, take a long time to compute. Finally they are by no means biologically plausible. We tried to implement a simple stereopsis algorithm based on the principle of finding corresponding points in the left and right visual fields and overestimating distances in conflictual situations. However this was not concluant because OpenGl distortions and lighting calculus strongly impaired the similarity between the left and right image of the same point, and there were always a false pixel in the distance map.

Neural network for the snapping task

When the salamander fixates it prey before snapping, the stimulus is present in both tectal hemispheres. Moreover its image shifts to the rostral part of the optic tectum as the prey comes closer (see figure 4.15). By summing the **rostral** tectal activity (of both tectal hemispheres) we have a good estimation of the prey proximity. The projection mapping is shown in figure 4.16. This model is efficient with respect to the numbers of neurons involved as it is based upon divergent patterns of the tectal neurons described previously. Performance results are presented in section 5.3.

4.7 Behavior Algorithm

We use a very simple behavior algorithm. With respect to the behavioral data presented in section 2.2.2, the animal orients his head toward the prey, fixates at it binocularly, approaches the prey and finally snaps at it when it is in the tongue reach. If a predator occurs somewhere in the visual field, the animal

Figure 4.14: Representation of the same stimulus at different distances. A 16 mm stimulus moves at 15 mm, 30 mm, 50 mm, 100 mm and 150 mm in front of the salamander.

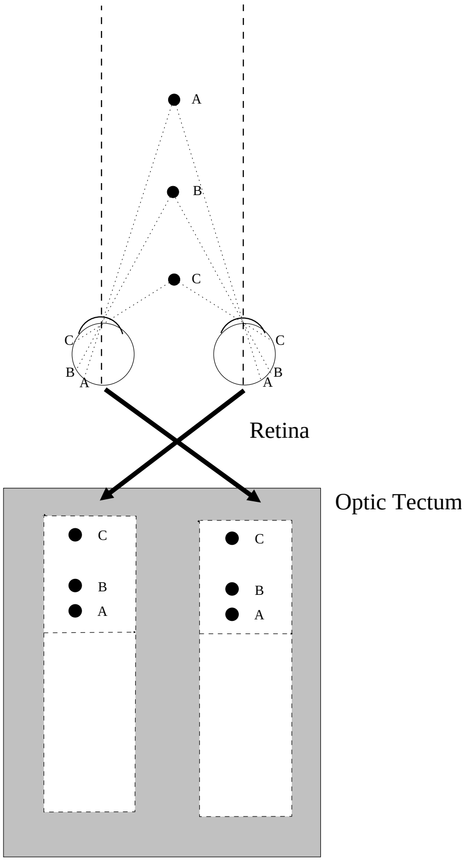

Figure 4.15: Objects at different frontal distances stimulate the tectum in different ways. The more close is the stimulus, the more its image is represented rostrally in the tectum (near -45°).

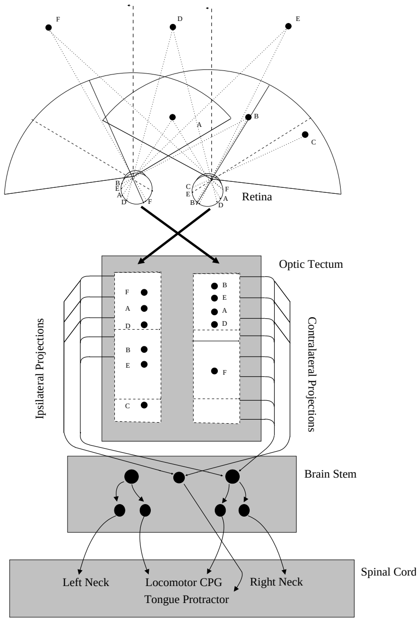

Figure 4.16: Divergent projection patterns from the tectum. Rostrally positioned neurons stimulate the tongue protractor.

stops the feeding sequence and flees for a determined moment of time (i.e., escape behavior is prioritary as it is a matter of life and death). This can be achieved using concurrently active *Orienting*, *Approaching*, *Snapping* and *Escape Schemas* for tongue, neck and body muscles control (for an introduction on *Schema* theory please refer to [1]). Orienting, Approaching and Snapping Schemas are driven by tectal signals as described in sections 4.3 and 4.6. As the salamander performs orienting movements with its head only, the approaching schema is inhibited by the orienting schema (i.e., body tonic drive is suppressed for larger orienting angles). The snapping schema works independently. The escape schema is driven by pretectal signals (see section 4.5) and inhibits all preceding schemas when its activity is above a certain level.

4.8 Additional Programming Work

The *Salamander* project being incremental (i.e., new extensions are frequently added to account for more complete behavior and each time new neural networks are incorporated within the existent networks), the use of an oriented-object programming language seemed most appropriate. Therefore we implemented a **C++ version** of the salamander simulator (initially written in C). To facilitate the creation of more realistic and complex environments in the simulator, we implemented the possibility to **import textures** from image files[7]. Finally we implemented a stable procedure for **creating AVI movies** from the simulation.

---

[7] OpenGl demands images files with dimensions that are power of two.

Chapter 5

Results

In this section we present results about the models presented in the previous section. **Films** of almost all the experiments can be found on `http://birg.epfl.ch/`[1] with the following link: student projects, projects pages, B.Petreska.

5.1 Experiments

The two optic tectum models described in section 4.3 were "trained" (i.e., optimal values for α^c, β^c, α^i and β^i were defined, through an exhaustive search of the parameter space) for the specific task of head orienting. The model was subsequently tested in situations other than the experimental conditions. We were particularly interested in gaining more understanding in the model behavior and in evaluating its robustness to a change in the environmental scene (i.e., different stimulus size, different background, etc.).

We also "trained" the network for complex environments. Distracting objects were added on the background (see figure 5.11), which resulted in considerable noise in the tectum activity (i.e., noise is defined as a non-stimulus activity). The idea was to search whether weights optimal for both simple and complex backgrounds existed, or whether the network specialized for a particular configuration of the visual input.

In a second phase we investigated whether the same weights were optimal for a purely orienting (i.e., large head movements based only on contralateral input) and gaze stabilization (i.e., small orienting angles with contralateral and substantial ipsilateral visual input) behaviors.

The next step was integrating approaching behavior, pretectum and snapping models. Respective results are discussed in the remainder of the section.

Finally we reproduced several lesion and behavioral experiments to see if the model could account for the biological data presented in section 2.

5.1.1 Experimental Conditions for the Orienting Behavior

A 28cm salamander was placed in the middle of a (2m x 2m x 2m) three-dimensional box. The size of the box is largely sufficient as salamanders are nearsighted animals.

---

[1] http://birg.epfl.ch/page43419.html.

We reproduced the Ewert experiment, where the stimulus is moved with a constant speed in front of the animal. The stimulus moved on a semi-circular trajectory, at a constant distance from the salamander, from left to right. The latter has no incidence on our model as weights were attributed symmetrically (side preferences are not significant in salamanders [29]). The stimulus entered in the salamander's visual field from the left (eccentricity of 100°), which optimally induced a large orienting movement to the left. Then the salamander had to fixate the stimulus binocularly, as it traversed the visual field to the right. The salamander's body was stationery, all motoneurons other than the neck were inhibited.

We argue that if the salamander is able to follow a constant-speed movement for different values of velocities, it shall have no difficulty in tracking an irregularly moving stimulus within the same range of velocities. If our model can cope with different values of speed, then it can also cope with a speed-varying stimulus as long as its speed stays in the good range. Moreover [18] demonstrated that the locomotor CPG could produce stable rhythmic patterns despite the rapidly changing input signals. The model was tested with a randomly-moving stimulus.

Many relevant parameters had to be fixed. For choosing their values we followed two principles. The first one was to use biologically motivated optimal values and the second was to simplify when possible. Thus the *stimulus size* was fixed to 16 mm, which at the *distance* of 22 cm, corresponded to 4° of the visual field (we used *S.salamandra* preferred angular and absolute prey-sizes (see Table 2.1)). The stimulus was moved with a prey *velocity* of 20°/s, which is the highest optimal value found in literature (see Table 2.1). We used a black stimulus on a white background, as it is usually done in behavioral experiments. The total number of *retinal ganglion cells* of type 2 only was 20 298, and the number of tectal cells was 2 255. However the number of peripheral cells was overestimated (see figure 4.1). One tectal column contained only 66 neurons (which corresponds to a neuron every 2.2° of visual field[2]). Every experiment's results were accompanied by a file descriptive that state the values of the fixed parameters.

5.1.2 Exploring the parameter space

Weights were determined through an exhaustive search of the parameter space. We first defined the plausible intervals for α^c, β^c, α^i and β^i parameters of the contralateral and ipsilateral linear weight functions:

$$\omega^c(\theta) = \alpha^c\theta + \beta^c \tag{5.1}$$

$$\omega^i(\theta) = \alpha^i\theta + \beta^i \tag{5.2}$$

where θ is the horizontal angular distance of the tectum neurons. Thus, the minimal value that provoked uncontrollable head movements and the maximal value that did not elicit any orienting movement were assigned as limits of our search space. We then tried many combinations of parameter values each time refining the areas containing the best results. See figure 5.1 for the distribution of error after a first exhaustive search of the parameter space (for 20

---

[2] The visual field for one eye is 145°.

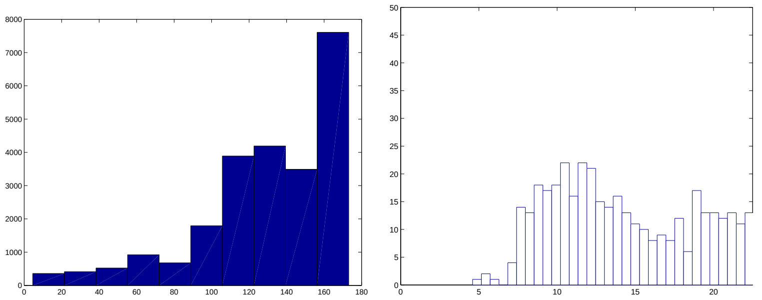

Figure 5.1: Distribution of errors with 20 000 simulation runs. The error is defined as the difference between the orienting angle of the salamander and the real stimulus angle. A detail of the distribution of minimal errors is shown on the left.

000 combinations). We searched for positive α^c and negative α^i values, as the contralateral and ipsilateral visual inputs come from a different eye and should induce an orienting movement to the same direction. The offset values could be either positive or negative.

To evaluate the different parameter combinations we considered the difference between the induced orienting movement and the real stimulus direction. We kept the combinations that minimized this error. We ran many different experiments, however the most significant results will be presented.

5.1.3 First Tectum Model

Salamanders with tectum model as described by equations 4.6 in section 4.3 follow the stimulus prey with high accuracy. However as predicted, they are not stable with respect to change of the experimental environment. Increasing the stimulus size increases the motoneuron activity and the salamander head starts oscillating around the correct angle as the orienting angle is overestimated (i.e., the salamander turns his head too much to the right and then the stimulus is on its left, etc..).

5.1.4 Second Model

In this section we present the results about the tectum model described by equations 4.9 in section 4.3

Reaction to stimulus parameters

The model is robust to any change of the stimulus parameters. The precision is not impaired with increasing stimulus size, as was the case in the previous model (see figure 5.2, left). The minimal size that elicits orienting is 2mm (as in table 2.1). Very small sizes fail to stimulate sufficient tectum activity, but do elicit orienting behavior. The model is accurate at following slowly moving stimulus, and the error increases with increasing velocities (see figure 5.2, right). Objects very close to the salamanders provoke errors, as the salamander can not exactly perceive their contours (i.e., a close object covers a large area of the visual field)

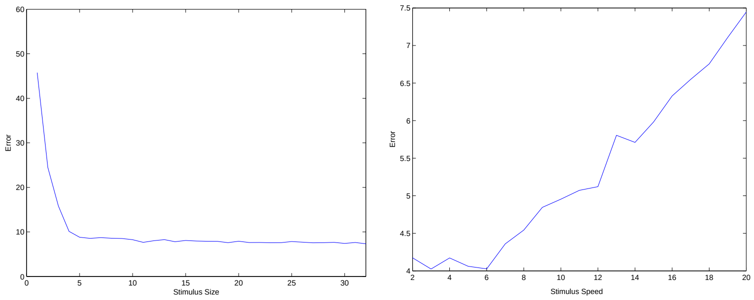

Figure 5.2: On the left. The model supports different sizes of objects. The stimulus size is in mm, and the error in degrees of visual field. On the right. Following a stimulus at different velocities (in °/s).

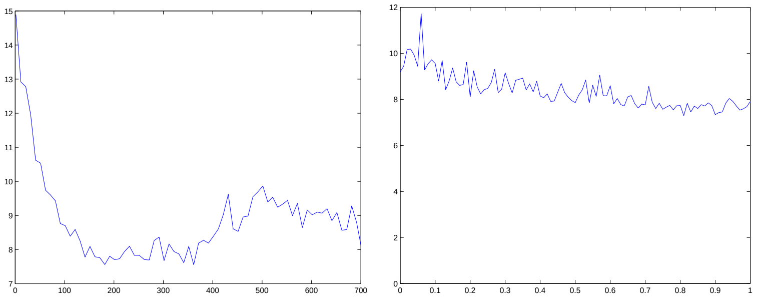

Figure 5.3: On the left. Reaction of the network to change of the stimulus (in mm). On the right. Reaction of the network to change in contrast.

and distant objects provoke errors du to their small appearance (i.e., this is consistent with our results on the stimulus size, as shown on figure 5.3, left). The accuracy is not impaired with changing contrast. Good results at very low contrast are also du to OpenGl which shades the stimulus object (see figure 5.3, right).

The error presented on the y axis in the figures is not the minimal error for fixating moving objects, for it also accounts for the error induced while getting the stimulus in the binocular field in the first place. Therefore it should not be interpreted as measure of precision.

5.1.5 Analyze of parameters α and β

For the results presented in this section we used the second tectum model described by equations 4.9 in section 4.3. Several combinations of values gave similar results. Retained optimal values are given in Table 5.1. The graph of the weights functions (equations 4.7 and 4.8) is shown on figure 5.4.

Once we had determined the optimal values for the weights function parameters, we plotted several interdependencies in order to gain more understanding on α and β parameters.

	$\alpha_{contralateral}$	$\beta_{contralateral}$	$\alpha_{ipsilateral}$	$\beta_{ipsilateral}$
Value	9.4×10^5	0.0015	-1.4×10^{-4}	0

Table 5.1: Best values for the weight functions parameters.

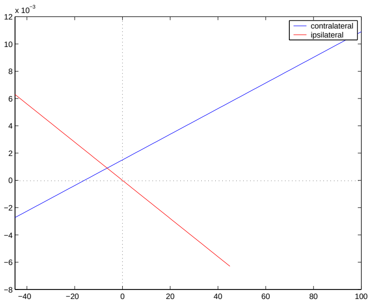

Figure 5.4: Optimal contralateral (in blue) and ipsilateral (in red) weights linear functions. The ipsilateral input covers only the binocular field (from -45° to 45°) and the contralateral input covers the whole visual filed (from -45° to 100°, for a horizontal and binocular visual fields of 200° and 45° respectively)

α Parameters

From what we can observe in figure 5.5, the area of minimal error (in black) is well defined and rather large. This could explain the multitude of different combinations with similar performance. We observe that for values close to zero (upper left corner) the result is bad. The reason for this is that the orienting response is too low with respect to the correct angle (i.e., $\alpha^{*}\theta$ is too small). From the minimal error zone we can derive the appropriate intervals for $\alpha_{contralateral}$ and $\alpha_{ipsilateral}$ (i.e., they are of similar sizes, about 1.5×10^{-4}). Contralateral and ipsilateral α best values are in the same range of values, however, they influence each other (observe the oblique form of the black area). For other *beta* values (i.e., than optimal), the picture is about the same, but the intervals are shifted. In figure 5.6 (i.e., plot of $\alpha_{contralateral}$ and $\alpha_{ipsilateral}$ with different β values) we can observe the same configuration as the in figure 5.5 (i.e., a zoom is applied compared to the latter).

β Parameters

From figure (5.6) we can observe that optimal values are situated in the area near zero values. This is rather logical, as an important positive offset, would elicit a positive value for negative values of θ (i.e., the part of the binocular field which is on the other side of the monocular). This would involve a temporal turn (see figure 2.3, right) instead of turning to the nasal side. The model is less sensitive to changes in $\beta_{ipsilateral}$ than $\beta_{contralateral}$ (the minimal error area is vertically extended). This as well is coherent as ipsilateral weights function applies to a restrained part of the visual field (i.e., binocular) compared to contralateral which extends to the whole visual field. To our opinion *beta* parameters are not essential to the model, as suppressing them yields similar accuracy (see minimal error area range of values in figure 5.7).

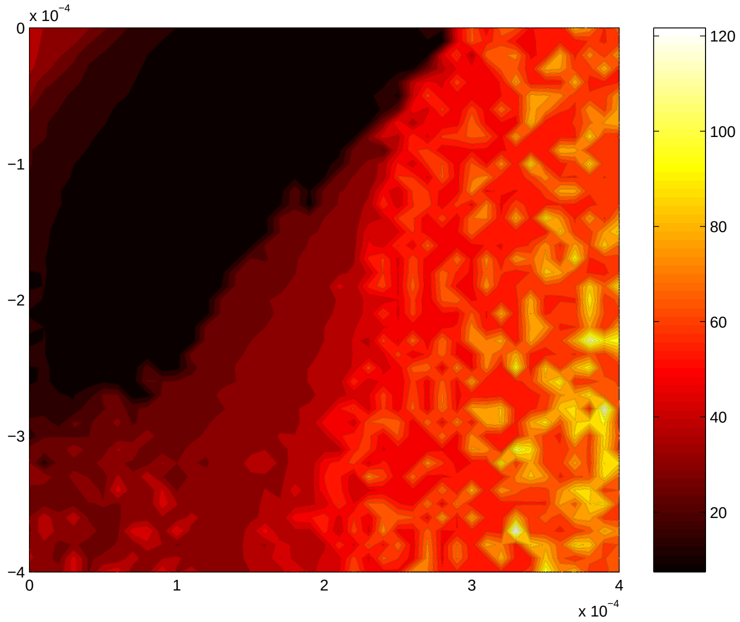

Figure 5.5: Graph of $\alpha_{contralateral}$ (x-axis) and $\alpha_{ipsilateral}$ (y-axis) with optimal β values. Point (0,0) is in the upper left corner. Minimal errors are in black.

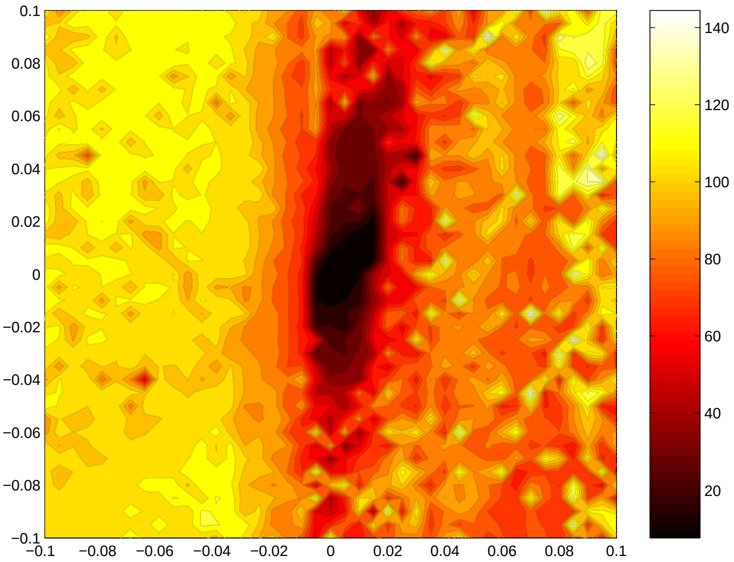

Figure 5.6: Graph of $\beta_{contralateral}$ (x-axis) and $\beta_{ipsilateral}$ (y-axis) with optimal α values. Minimal error is represented in black.

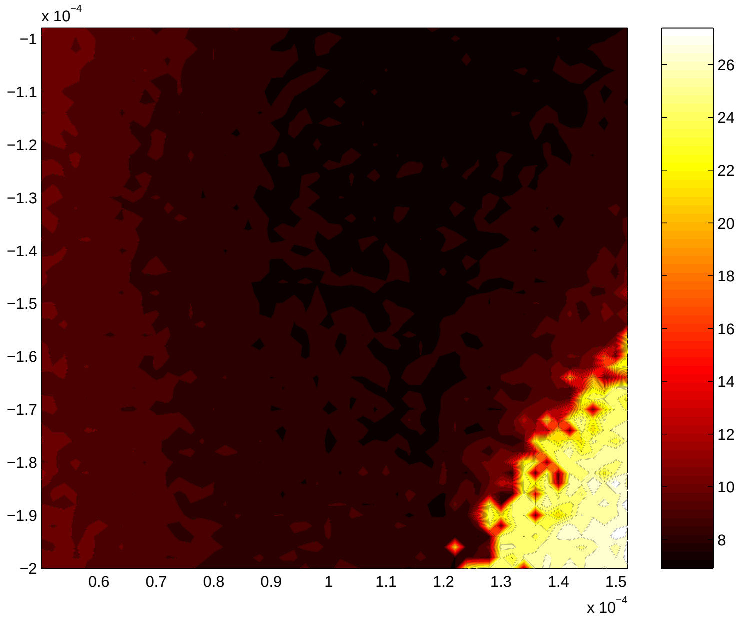

Figure 5.7: Graph of $\alpha_{contralateral}$ and $\alpha_{ipsilateral}$ with no offset ($\beta_c = 0$ and β_i=0). Minimal error is represented in black.

Without ipsilateral input

Salamander species like *S.Salamandra* receive predominantly contralateral retinal input. We investigated whether the model without ipsilateral input presented in section 4.3, by equation 4.4, can also generate correct orienting angles. This indeed is the case if you observe the minimal error area values (in black) on figure 5.8. Here as well we constat that *beta* values are not essential (minimal error zone is near *beta* = 0).

With monocular input

We observe similar configurations as in the previous sections, with a much more regular pattern (see figure 5.9). The dark red zone in the second graph corresponds to too strong orienting to the left in the beginning of the experiment, such that the stimulus gets out of sight, and the salamander does not react anymore.

5.1.6 Increasing the accuracy

When the salamander followed the prey with his head, he was late with respect to the stimulus movement. This delay was attributed to the muscles activity. However we ran *gaze-stabilization* specific experiments to see if we could compensate this lateness. We discovered that the optimal values for fixating were much higher than those found in section 5.1.5. But when we ran the simulations with the gaze-stabilization best values, the large-angle orienting movements were obviously too strong. Actually the values found in section 5.1.5

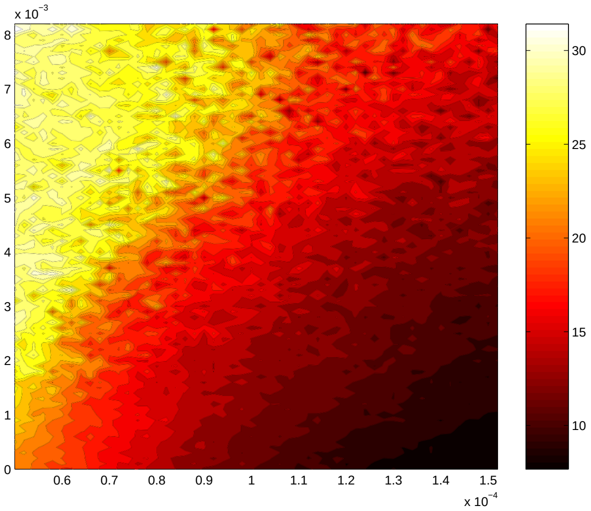

Figure 5.8: Graph of $\alpha_{contralateral}$ (x-axis) and $\beta_{contralateral}$ (y-axis). No ipsilateral input.

are a compromise between gaze stabilization and orienting with large angles optimums. Therefore we defined different contralateral α and β parameters for the binocular field and monocular fields. The new values are summarized in Table 5.2. The graph of the new weights function is shown in figure 5.10. The difficulty with this approach are the oscillating movements of the salamander (du to the high parameter values), which have to be suppressed augmenting the damping parameter for the neck muscle activity. With this model we achieve an accuracy of less than 2° for low speeds (in average, as the salamander follows the prey with a saccadic movement). However the model is less robust to environmental changes.

$\alpha^c_{monocular}$	$\beta^c_{monocular}$	$\alpha^c_{binocular}$	$\beta^c_{binocular}$	$\alpha_{ipsilateral}$	$\beta_{ipsilateral}$
8×10^4	0.0001	1.6×10^4	0.002	-1.8×10^{-4}	0

Table 5.2: Best values for the separated weights functions parameters.

This model showed best accuracy results, gaining from 1° to 2° in precision for gaze stabilization. This model is particularly interesting because in a way it gives more credit to the frontal area than to the temporal area of the visual field (i.e., it presents a sort of *spotlight* feature). It might well constitute a pseudo visual attention mechanism (visual attention consists of locally amplifying (by backprojection) the retinal signal, in points that are more relevant, such as a prey position). When the salamander follows a prey stimulus it never changes for another target, even if it presents a more favorable configuration (see section 2.2.1).

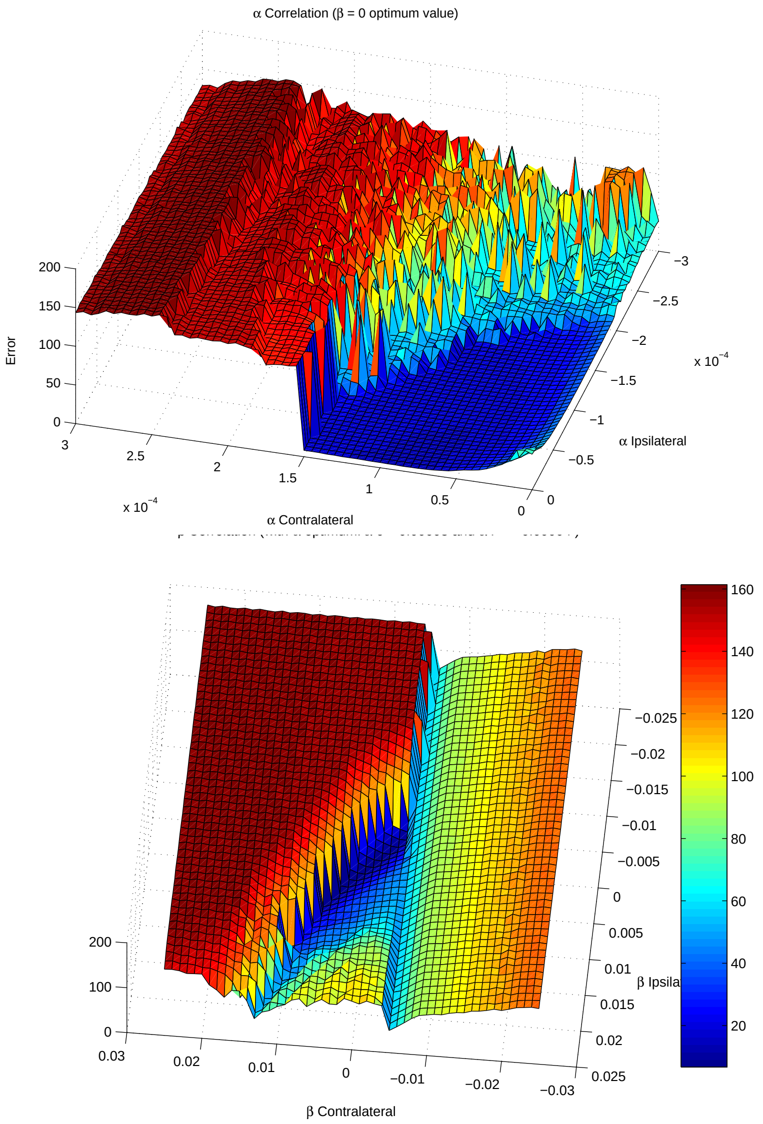

Figure 5.9: Graphs of $\alpha_{contralateral}$ (x-axis) and $\alpha_{ipsilateral}$ on top and $\beta_{contralateral}$ (x-axis) and $\beta_{contralateral}$ on bottom. With input from one eye only. The error is represented on the z-axis.

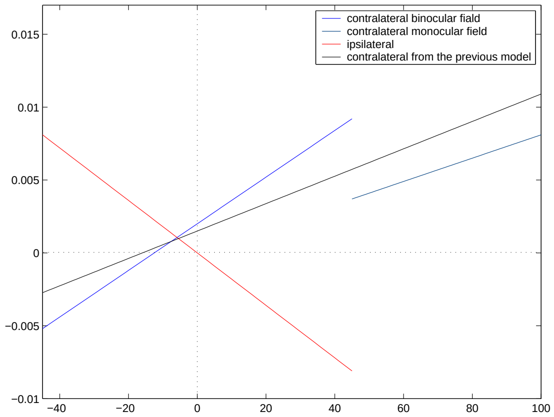

Figure 5.10: The use of two different contralateral weights functions (i.e., one for binocular and one for the monocular field, in blue). Experiences show that higher $alpha^c$ yield better accuracy in the frontal field but impair the accuracy for large orienting angles. The disposal of the two slopes indicates that probably a *continuous non-linea*r weights function is needed, that would take into account both optimal values.

5.1.7 Overlap and number of tectal cells

To our opinion the figure 2.5 on distribution of binocular tectal cells sizes is incomplete, since it does not differentiate between the types of the tectal neurons. We believe that the distribution of receptive fields sizes with respect to a particular tectal type is less variant (they are usually characterized by their wide or narrow dendritic fields, see section 2.3.2). The particular concentration of values around 120° and 180° and the important number of 180° receptive fields may well correspond to a particular cell type involved in specific overall calculations. However decreasing the tectal cells receptive fields sizes does impair the accuracy of our model, since one neuron corresponds to large areas in the visual field, and the salamander reacts when the stimulus enters an area represented by another neuron. The situation is redressed with the use of overlapping large receptive fields (i.e., small center and large surround receptive fields). Many large tectal and retinal cells respond best to 2-3° stimulus, indicating that the central receptive field is small. The use of 15° cells (with a central zone of 3°) impairs the precision by only 2°. The overlap produces diffuse activity patterns in the tectum.

5.1.8 With Background

With complex environment the salamander has some difficulties in following the prey as the amount of noise is considerable (see figure 5.11). This is not surprising as no selective or "winner-takes-all" mechanism was implemented. The salamander achieves to orient his head toward the stimuli every time the stimulus was "visible" (i.e., in front a sky background and not objects with similar color). With slow-moving stimuli, the salamander needs several saccades to bring the stimulus in its binocular field and then follows the stimulus with only

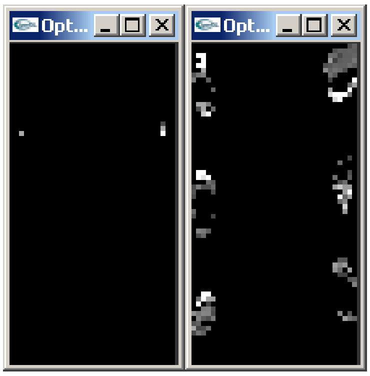

Figure 5.11: Difference between tectal activity with a simple stimulus and tectal activity with the same stimulus in a complex environment. Shows the amount of "noise" du to induced movement.

slightly impaired accuracy. The best weights function parameters for orienting movement with complex environment were higher than best values with single stimulus.

The salamander discriminates between two objects of same angular size and different absolute sizes. We observed that the existence of a second sphere moving coherently to the first (the spheres have the same size), makes the salamander deviate from the correct orientation (i.e., follows a sort of "average fly"). It usually prefers closer prey stimulus.

As expected the salamander does to some extent discriminate between different objects of same apparent angular size and between a static background and a moving stimulus. Ideally it should be coupled with another mechanism, such as visual attention.

5.2 The Pretectum Model

As shown on picture 5.16, the salamander discriminates between a small prey object and a large predator object. However the model is not perfect as it is based upon angular and not absolute size. This might also be the case in salamanders with a poor visual system (see section 4.5). We know that certain salamanders show size constancy up to 23cm, but we also know that tectal cells are sensitive only to angular size (see section 2.3.2). The fact that many salamanders have highly developed camouflage skills and poisonous gland secreting might also indicate that they do not utterly rely upon their visual sense as detecting predators is concerned.

In this model the threshold is essential, if it is too high it will not detect all predators, and if it is too low it will detect confuse prey and predator stimuli. However no data on salamanders predators could be found, therefore the threshold was fixed arbitrarily. The problem with this model is that a close-prey stimulus may be interpreted as a predator (i.e., they both have large angular size), however we override these ambiguous signals by the snapping signals, which represent a sort of "proximity" information. The "memory" neuron re-

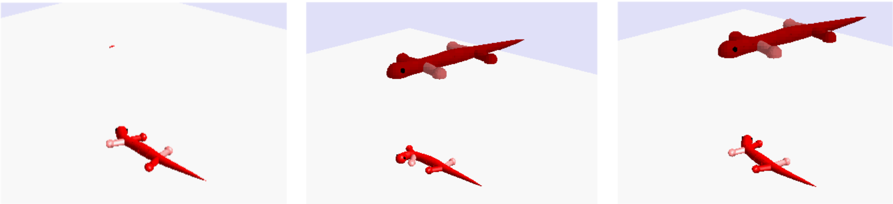

Figure 5.12: The salamander follows a prey object and escapes from a predator (left and middle). With pretectal lesions the salamander attacks at threatening stimuli (right).

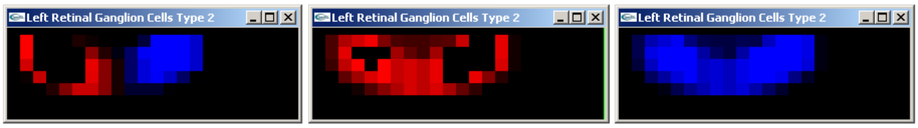

Figure 5.13: Separating ON and OFF changes in light intensity enable discrimination between objects that move away (in the middle) and approaching objects (on the right). In blue an OFF change, ON change in red. For more details see section 4.5

sponse that prolongs the pretectum activity determines the length of the "escape period".

To our deepest regrets we did not have time to test the temporonasal direction-sensitive movement neuron with respect to walking in a complex environment. Surprisingly the same mechanism can be used to discriminate between approaching and fading objects, which salamanders are capable of (see figure 5.13). When an object approaches, it increases in size and darkens a bigger part of the visual field, which results in predominant OFF-changes, the opposite occurs for objects that move away from the salamander.

5.3 The Snapping Model

The main advantage of this model, when compared to Simulander II (see section 3.3), is that it does not involve any additional neurons. It is based upon diverging projection patterns of the tectum, so the same tectal neurons involved in orienting behavior, control also the snapping behavior. Our model is consistent with the biological lesion data found on the subject. Destroying the tectum abolishes also the snapping reflexes and with smaller lesions, frogs responded to prey with an overshoot for distance that increased with the size of the lesion–suggesting that overall activity in the pathway codes for "closeness" rather than distance [4]. Our model predicts the same thing, since closer objects elicit higher motoneuron activity (i.e., they are positioned in the very rostral part approaching -45°) and distant objects elicit lower tongue protractor activity (i.e., in the tectum they are situated near 0°), as is shown on figure 4.15. In Simulander it is the opposite: an object that is far away elicits reaction in many tectum neurons [9], which is inconsistent with the biological data presented in [4] and is also inconsistent with our observations from the tectal activity. As a distant object seems smaller, his representation in the tectum affects less neurons than the same object closer.

The precision of our model is lower than in Simulander II (80-100%). We observe correct protraction length in about 30% with a non-optimized function, which is much more realistic (*S.salamandra* success rate in snapping is only 40%). The precision depends on the stimulus movement direction[3]), However it is limited to frontal tongue protraction only (this is also the case in Simulander II).

5.4 Behavior Schema

Integrating behavioral schemas was trivial for one stimulus environment. The salamander has no difficulty following the prey. However in a complex background the salamander seemed "frightened", it moved his head around in a non-organized way. We were unable to reduce the lateral head movements induced by the locomotor circuit (it provoked deviations from the correct angle up to 15° laterally, on each side). From what we have seen from [3], salamanders have a stable approach, with minimal head movements. We suggest that the neuromechanical model needs to be modified in order to suppress these annoying oscillations.

5.5 Lesion and Stimulation Experiments

The following lesion experiments (see section 2.3.5) are reproduced by our model: 1) lesion of the tectum abolishes any response to a stimulus present in the scotoma field; 2) stimulation of the tectum triggers exaggerated avoidance movements (our model predicts large head movements in the stimulus direction[4], since orienting is overestimated, we have no indication on the exaggerated avoidance movements mentioned in [26]); 3) lesion of the pretectum results in feeding disinhibition as shown on the third picture in figure 5.16.

5.6 Reproduced Behavior

In this section we present several emergent proprieties (i.e., behavior that was not considered when constructing the network model, but perfectly corresponds to behavioral data).

5.6.1 Generation of saccadic movements

We observed the same saccadic head movements as in salamanders. During pursuit movements the head accelerates for a few seconds, until maximum velocity is reached, and then is released. We attribute this saccadic movements

---

[3] We do not know whether this is also the case in real salamanders.

[4] High excitation triggers oscillatory movements. The orienting angle being overestimated, the stimulus is then visible on the opposite side, which triggers an opposite orienting movement, etc.

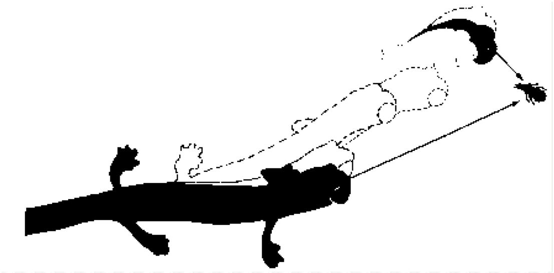

Figure 5.14: With one eye covered *Hydromantes Italicus* shows a conspicuous approach behavior toward a prey. It takes a curved path to approach the prey and bends his body away of it toward the side of the seeing eye, compensating the bending by turning the head between 60° and 90°. Bottom picture, our salamanders shows the same behavior.

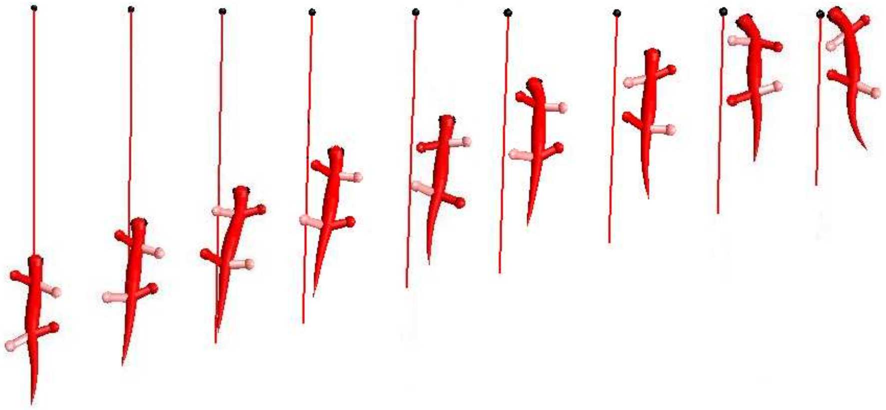

Figure 5.15: Our monocularized salamander exhibits the same approach behavior as in figure 5.14.

to the network resolution. The salamander starts an orienting movement when the prey enters the receptive field of another neuron and stops the orienting movement stops when the prey has been positioned back in the frontal visual field.

5.6.2 Monocularized Salamanders

In monocularized experiments (i.e. when one of the eyes is removed), the modelling results also agree with behavioral experiments. Monocular salamanders take a curved trajectory with a stronger bending of the head compared to the intact approach as shown on figure 5.9.

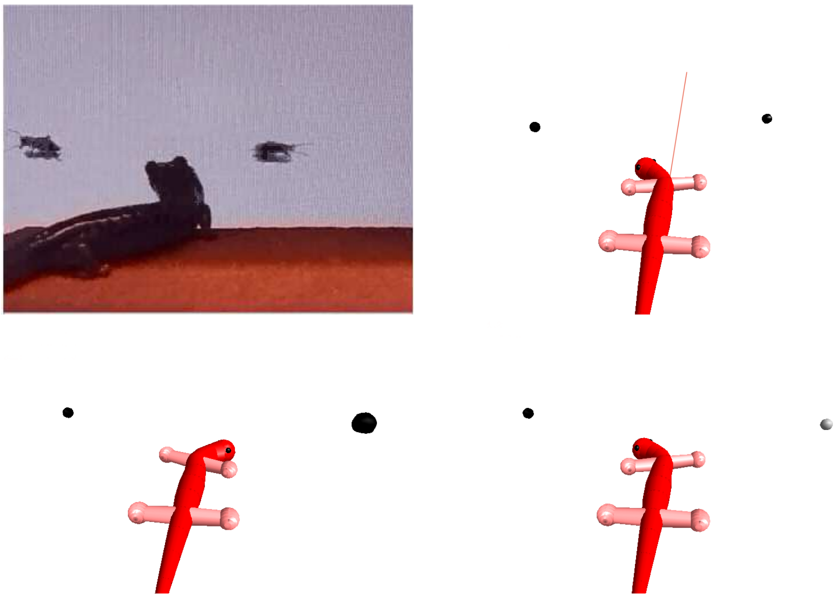

Figure 5.16: As in real experiments, the salamander prefers faster, bigger and objects of higher contrast. The salamander makes the decision only upon its own perception.

5.6.3 Prey Preferences

The experiment with double stimulus was reproduced. Just like real salamanders (see 2.2.3), our salamander (after a little "hesitation") prefers larger stimuli and preys of higher contrast. We insist on the fact that the salamander makes its decision upon its own sensory perception. In Simulander, the visual input to the tectum is a function of the stimulus size and the stimulus velocity (i.e., corresponds to the observer knowledge). We made our model contrast-sensitive by using a linear difference function (rather than binary) for the retinal ganglion cells of type 2. The salamander prefers larger prey objects since they enhance larger activation areas in the tectum.

Faster objects are also preferred. They activate higher activity in the tectum (as they achieve larger eccentricity angles in less time). However for certain speeds, the salamander turns back to the slower stimulus, as suddenly it is projected to the peripheral visual field. This artefact would be completely suppressed by a visual attention mechanism.

5.7 Relevant Topics

5.7.1 Visual Acuity

Despite the low number of retinal ganglion and tectal cells, and despite the localization precision of about 3°, the salamander had no difficulty with orienting its head toward a minimal size stimulus, such as 0.5mm at a 50mm distance (which was falsely used in [9] to prove that the number of tectal cells needed was immense (see section 4.3)). Even though the stimulus is barely visible, as the tectal signal is normalized, it is sufficient to trigger correct orienting nead movements.

5.7.2 Reaction to stationery prey

When stationery the salamander never responds to a stationery stimulus. However when walking, du to self-induced movements (see sections 2.5 and 5.1.8), it does not discriminate between stationery and moving prey.

5.7.3 Comparison with Simulander

Simulander I [7] is a feedforward neural network, simulating the orientation movement of salamanders, based upon coarse coding mechanisms (see section 3.2). They use only 100 neurons. However their stimulus space is situated only in the frontal visual field of the salamander. The number of neurons used in our implementation is higher (around 2000 with an overestimation of the peripheral visual field), but still biologically plausible (3300 descending projection neurons in H.Italicus). Our model is less accurate (average error of less than 3° for slowly moving, and 6° for high-speed stimulus), but more realistic. It fits within biological data values in literature (3°). Simulander also shows preferences for fast and large objects, however this preference is based upon the observer's knowledge (i.e., the visual input is a function of the angular size and angular velocity). Our network reacts faster as it needs not more than two seconds to fixate a prey binocularly with an eccentricity of 100° (5s in simulander). Compared to Simulander, there are no particular positions in our model where stationery objects elicit orienting movements.

We would like to remind you that **movies** of almost all the experiments are available on the http://birg.epfl.ch/ website.

Chapter 6

Discussion

This work investigates the neural mechanisms underlying visually-guided behavior in salamanders, with a special attention to the interplay of neural processing and the biomechanics of the vertebrate body. We developed biologically motivated models of the retina, the optic tectum, the pretectum and the brain stem which were coupled to the spinal locomotor circuits and to the biomechanical model of a simulated salamander robot. The model integrates typical orienting, gaze stabilization, approaching and snapping behaviors specific to the salamander feeding activity.

We demonstrate how topological maps of neurons with large receptive fields in the optic tectum can be used to reproduce salamander approach behavior to stimuli in a neuromechanical simulation. With a simple structured mapping between the optic tectum and brainstem, the salamander is capable of tracking a simple prey stimulus with high accuracy. The parameters of the linear activation function have been defined through an exhaustive search of the parameter space. We suggest that the sensorimotor transformation that occurs from the tectum to the brainstem is that of the horizontal angular distance of tectum neurons to amount of muscle activity. The processed visual input directly stimulates the neck motoneurons. Moreover the numbers of neurons used is biologically plausible. The decision to normalize the visual signal has made the network robust to all change in the stimulus parameters. We also suggest that even simpler models entail similar accuracy (i.e., with only contralateral input or leaving aside the offset parameters).

We propose a potential mechanism for tongue protraction in *S.salamandra*, which reproduces realistic snapping success rates. The proposed circuitry is only hypothetical, and correctly predicts a "closeness" rather than distance coding. We also propose a simple prey-predator discrimination model that responds with escape or feeding behavior depending on the stimulus.

Induced movement is sufficient to perturb the model accuracy. However when one takes into account that no selective mechanism such as "winner-takes-all" had been implemented, the model performs well. No previous work had tackled the problem of multiple stimuli within the visual field. The effect of complex environment onto tectal activity is directly observable.

Simulations show that relatively simple mappings can reproduce a large amount of salamander neurophysiological and behavioral data. The deactivation of the different components accounts for investigations made in lesioned animals. We also observed the same saccadic movements in orienting behavior as those presented in literature. The model reproduces the particular curved path observed in monocularized salamanders and shows the same preferences as observed in real salamanders. We insist on the fact that the salamander bases its decisions only upon his own sensory perceptions (i.e., closed sensing-to-acting loop). To our knowledge it represents the most complete extant amphibian model.

However, there is no real depth mechanism in our model, as snapping behavior is restricted to the frontal area and prey-predator discrimination is based upon the angular size of the stimulus. The model also fails to respond to a complex environment, suggesting it should be coupled with a selective or visuo-attentional mechanism.

The simulation environment tool represents a perfect test bed for any hypothesis related to visuomotor coordination. It is particularly appropriate for it provides visual demonstrations (i.e., one can observe neural networks activities and the modeling results). Moreover it is highly extendable.

When thrown in the real world our salamander resembles a little new born. This makes us feel it is only a beginning.

Chapter 7

Future Work

Future research efforts could be extended in a multitude of directions. The presented models could be improved using nonlinear weights functions and more realistic neuron distribution and density. The use of time-dynamical leaky-integrator neurons could be investigated as well. The effect of overlapping receptive fields should be studied in more depth. Models for visual attention [30] or experience-based behavior [31] could be developed and integrated to the previous. The brain areas such as the nucleus isthmi and particularly the thalamus (involved in obstacle avoidance) should be also modelled in order to account for even more complex behavior. Finally priority should be given to exploring more complex depth estimation and object-background discrimination mechanisms.

Acknowledgments

First and foremost I am deeply indebted to my family. I am indeed very grateful to Professor Auke Jan Ijspeert for letting me work on such a motivating subject and for his valuable advice throughout the work as well. I also wish to thank Ludovic Righetti for his infallible support. Many thanks to Alessandro Crespi who always had time to tackle several annoying problems. Thanks to all my friends. I very much enjoyed the company of all the master thesis students and the welcome of the Logic Systems Laboratory was exemplary!

Bibliography

[1] M. A. Arbib. Visuomotor coordination: neural models and perceptual robotics. *Visuomotor Coordination*, pages 121–171, 1989.

[2] M. J. Berry, I. H. Brivanlou, T. A. Jordan, and M. Meister. Anticipation of moving stimuli by the retina. *Nature*, 398:334–338, 1999.

[3] CNRS, editor. *Le Triton et la Salamandre.* 1996. video tape.

[4] A. Cobas and M. Arbib. Prey-catching and predator-avoidance in frog and toad: defining the schemas. *Journal of Theoretical Biology*, 157:271–304, 1992.

[5] S. M. Deban and U. Dicke. Motor control of tongue movement during prey capture in plethodontid salamanders. *The journal of experimantal biology*, 202:3699–3714, 1999.

[6] U. Dicke. Morphology, axonal projection pattern, and response types of tectal neurons in plethodontid salamanders, i.: Tracer study of projection neurons and their pathways. *The Journal of Comparative Neurology*, 404:473–488, 1999.

[7] W.C. Eurich, G. Roth, H. Schwegler, and W. Wiggers. Simulander: A neural network model for the orientation movement of salamanders. *Journal of Comparative Physiology A*, 176:379–389, 1995.

[8] W.C. Eurich and H. Schwegler. Coarse coding: calculation of the resolution achieved by a population of large receptive field neurons. *Biological Cybernetics*, 76:357–363, 1997.

[9] W.C. Eurich, H. Schwegler, and R. Woesler. Coarse coding: applications to the visual system of salamanders. *Biological Cybernetics*, 77:41–47, 1997.

[10] Salamander feeding movies.
http://autodax.net/feedingmovieindex.html.

[11] D. A. Forsyth and J. Ponce. *Computer vision : a modern approach.* Prentice Hall, 2002.

[12] W. Gerstner. *Réseaux de neurones artificiels.* 2002.

[13] Visually guided behavior in salamanders.
http://www.klab.caltech.edu/ pam/behav.html.

[14] S. Haykin. *Neural Networks. A Comprehensive Foundation.* Prentice Hall, 1999.

[15] U. Heiden and G. Roth. Retina and optic tectum in amhibians: A mathematical model and simulation studies. *Visuomotor coordination: amphibians, comparisons, models, and robots*, pages 243–267, 1989.

[16] A. J. Ijspeert. A salamander paradigm for vertebrate visuomotor coordination: A neuromechanical model.

[17] A. J. Ijspeert. A connectionist central pattern generator for the aquatic and terrestrial gaits of a simulated salamander. *Biological Cybernetics*, 84(5):331–348, 2001.

[18] A.J. Ijspeert and M. Arbib. Visual tracking in simulated salamander locomotion. In J.A. Meyer, A. Berthoz, D. Floreano, H. Roitblat, and S.W. Wilson, editors, *Proceedings of the Sixth International Conference of The Society for Adaptive Behavior (SAB2000)*, pages 88–97. MIT Press, 2000.

[19] R. Jain, R. Kasturi, and B. G. Schunck. *Machine Vision.* McGraw-Hill, 1995.

[20] H. Kahl, H. Luksch, W. Wiggers, and G. Roth. The pretectum of urodele amphibians: An intracellular study on anatomy, connectivity and physiology of pretectal neurons in-vitro. In N. Elsner and H. U. Schnitzler, editors, *Brain and Evolution*, Thieme, Stuttgart, New York, 1996.

[21] H. Kolb. How the retina works. *American Scientist*, 91:28–35, 2003.

[22] H. Luksch, H. Kahl, W. Wiggers, and G. Roth. The pretectum of salamanders : An intracellular study on the morphology and physiology of pretectal neurons and their influence on tectal evoked potentials. In Burrows M., T. Matheson, T.L. Newland, and H. Schuppe, editors, *Proc. of the 4th Intern. Con. Neuroethol*, Thieme, Stuttgart, New York, 1995.

[23] H. Luksch, H. Kahl, W. Wiggers, and G. Roth. Connectivity of the salamander pretectum: an in-vitro (whole-brain) intracellular tracing study. *Cell and Tissue Researh*, 292:47–56, 1998.

[24] G. Manteuffel. Compensation of visual background motion in salamanders. In J.P. Ewert and M.A. Arbib, editors, *Visuomotor coordination: amphibians, comparisons, models, and robots*, pages 311–340. Plenum, New York, 1989.

[25] The organization of the retina and visual system. http://webvision.med.utah.edu/.

[26] G. Roth. *Visual behavior in salamanders.* Springer, Berlin Heidelberg New York, 1987.

[27] G. Roth, U. Dicke, and W. Grunwald. Morphology, axonal projection pattern, and response types of tetal neurons in plethodontid salamanders, ii.: Intracellular recording and labelling experiments. *The Journal of Comparative Neurology*, 404:489–504, 1999.

[28] G. Roth, U. Dicke, and W. Wiggers. Vision. In H. Heathwole, editor, *Amphibian Biology, Vol.3, Sensory Perception*, pages 783–877. Chipping Norton: Surrey, Beatty and Sons, 1998.

[29] N. Schülert and Dicke U. The effect of stimulus features on the visual orienting behavior of the salamander plethodon jordani. *Journal of Experimental Biology*, 205:241–251, 2002.

[30] Animat vision: active vision in artificial animals. http://mrl.nyu.edu/ dt/animat vision/.

[31] D. Wang and A. Arbib. Hierarchical dishabituation of visual discrimination in toads. pages 77–86, Paris, 1991. MIT-Press.

[32] D. Wegener and W. Wiggers. Projection specifity of retinal ganglion cells in salamanders of the family plethodontidae. In N. Elsner and H. Waessle, editors, *From Membrane to Mind*, Thieme, Stuttgart, New York, 1997.

[33] W. Wiggers. Topology and fine structure of visual projectins in the tectum of plethodontid salamanders. In N. Elsner and H. Waessle, editors, *From Membrane to Mind*, Thieme, Stuttgart, New York, 1997.

[34] W. Wiggers. Isthmotectal connections in plethodontid salamanders. *The Journal of Comparative Neurology*, 395:261–272, 1998.

[35] W. Wiggers. Projections of single retinal ganglion cells to the visual centers: An intracellular staining study in a plethodontid salamander. *Visual Neuroscience*, 16:435–447, 1999.

[36] W. Wiggers and G. Roth. Anatomy, neurophysiology and functional aspects of the nucleus isthmi in salamanders of the family plethodontidae. *J Comp Physiol A*, 169:165–176, 1991.

[37] W. Wiggers, G. Roth, C. Eurich, and A. Straub. Binocular depth perception mechanisms in tongue-projecting salamanders. *J. Comp. Physiol. A*, 176:365–377, 1995.

[38] Woesler. Object segmentation model: analytical results and biological implications. *Biological Cybernetics*, 85:203–210, 2001.

[39] R. Woesler, G. Roth, H. Schwegler, and C.W. Eurich. Mechanisms of object segmentation in the visual system of salamanders. In Preparation.

[40] S. Zeki. *A Vision of the Brain.* Blackwell Science, 1995.